

CHAPTER 7 GEOLOGY

CONTENTS

CHAPTER 7	GEOLOGY	7-1
7.1	Outline of the Geology of the Project Area	7-1
7.2	Geological Investigation Works.....	7-2
7.2.1	Previous Investigation Works.....	7-2
7.2.2	Geological Investigation Works carried out in the Study.....	7-3
7.3	Site Geology	7-4
7.3.1	Reservoir	7-4
7.3.2	Dam	7-7
7.3.3	Waterway and Powerhouse (Option-II).....	7-15
7.3.4	Waterway and Powerhouse (Option-III b).....	7-17
7.3.5	Estimated Mechanical Properties of the Foundation Rock	7-19
7.4	Construction Material	7-24

LIST OF TABLES

Table 7.2.1-1	Investigation Drillings carried out by NEA on 2000	7-2
Table 7.2.2-1	Investigation Drillings carried out in the Study	7-3
Table 7.3.2-1	Standard of Rock Mass Classification (for Drilled Core).....	7-9
Table 7.3.2-2	Standard of Rock Mass Evaluation.....	7-9
Table 7.3.2-3	Results of the Lugeon Tests at the Damsite	7-12
Table 7.3.3-1	RMR of the Underground Powerhouse of Option-II	7-17
Table 7.3.5-1	Physical Properties of the Drilled Core	7-20
Table 7.3.5-2	Tensile Strength of the Drilled Core	7-20
Table 7.3.5-3	Uniaxial Compressive Strength of the Drilled Core	7-21
Table 7.3.5-4	Rock Mass Classification and Mechanical Properties	7-22
Table 7.3.5-5	Estimated Mechanical Properties of Foundation Rocks	7-23
Table 7.4-1	Investigation Area for Concrete Aggregate	7-24
Table 7.4.2	Test Results of the Concrete Aggregate (2001)	7-25
Table 7.4-3	Test Results of the Concrete Aggregate (2005)	7-25

LIST OF FIGURES

Fig. 7.1-1	Geologic Plan of Project Area	7-27
Fig. 7.3.1-1	Geologic Map of Reservoir Area (1/3)	7-29
Fig. 7.3.1-2	Geologic Map of Reservoir Area (2/3)	7-31
Fig. 7.3.1-3	Geologic Map of Reservoir Area (3/3)	7-33
Fig. 7.3.2-1	Geologic Plan of Damsite	7-35
Fig. 7.3.2-2	Geologic Section of Damsite (A-A)	7-37
Fig. 7.3.3-1	Geologic Profile of Waterway & Powerhouse (Option-II)	7-39
Fig. 7.3.4-1	Geologic Plan of Waterway & Powerhouse (Option-IIIb).....	7-41
Fig. 7.3.4-2	Geologic Profile of Waterway & Powerhouse (Option-IIIb).....	7-43
Fig. 7.3.4-3	Geologic Plan of Outlet of Tailrace (Option-IIIb)	7-45
Fig. 7.4-1	Location Map of Investigation for Concrete Aggregate	7-47

CHAPTER 7 GEOLOGY

7.1 Outline of the Geology of the Project Area

Nepal is divided into five tectonic provinces of Tibetan-Techys zone, Higher Himalayan zone, Lesser Himalayan zone, Sub-Himalayan zone and Terai zone from north to south.

- Tibetan-Techys zone is the northernmost tectonic provinces of Nepal. It consists of Paleozoic to Paleogene sedimentary rocks such as shale, limestone and sandstone. Most of the Great Himalayan peaks of Nepal including Mt. Everest, Manaslu, Annapuruna belong to this tectonic province.
- Higher Himalayan zone is located in the below and the south of Tibetan-Techys zone. It is composed mainly of metamorphic rock such as gneiss, schist, marble, and some granitic rocks. Higher Himalayan zone contacts with Lesser Himalayan zone at Main Central Thrust (MCT) in the southern area.
- Lesser Himalayan zone is a broad tectonic province with numerous thrusts and nappes between Higher Himalayan zone and Sub-Himalayan zone. Main Central Thrust (MCT) is the boundary between Lesser Himalayan zone and Higher Himalayan zone in northern area, and Main Boundary Thrust (MBT) is the contact with Sub-Himalayan zone in southern area. Lesser Himalayan zone is composed of Pre-Cambrian to Neogene sedimentary rocks and metamorphic rocks such as slate, phyllite, quartzite, limestone and dolomite.
- Sub-Himalayan zone is a tectonic province bounded by Main Boundary Thrust (MBT) in north and Himalayan Frontal Thrust (HFT) in south. It consists of Neogene sedimentary rocks dipping northward. The lower portion of Sub-Himalayan zone is composed of siltstone, sandstone and mudstone, the middle portion of the zone is composed of medium to coarse grained sandstone, and the upper portion of the zone consists of conglomerate.
- Terai zone forms southern margin of Nepal and consists mainly of alluvial deposit.

Among five tectonic provinces mentioned above, Upper Seti Project area is located in the Lesser Himalayan zone where Pre-Cambrian to Paleozoic Nourpul formation, Dhading Dolomite and Benighat slate belonging to Nawakot group are distributed as shown in **Fig.7.1-1**. Nourpul formation and Dhading dolomite are late Pre-Cambrian to early Paleozoic in age and are composed of dolomite, slate, phyllite, quartzite, dolomitic quartzite and quartzitic phyllite. Benighat slate is late Paleozoic in age and consists of slate, phyllite, calcareous slate and a small amount of quartzite. These strata trend E-W to WNW-ESE, namely parallel to the Seti River, and dip southward.

7.2 Geological Investigation Works

7.2.1 Previous Investigation Works

The geological investigation works concerning the Upper Seti Hydroelectric Project were carried out by NEA (Nepal Electricity Authority) in 2000, and the investigation result was summarized in the Report on the Feasibility Study of Upper Seti Storage Hydroelectric Project, July 2001. The geologic investigation works carried out in 2000 are as follows;

a. Geological Reconnaissance

Area of Survey : Dam site, Powerhouse site, route of waterway and reservoir area

Scale of the map used : 1/1,000 (Dam & Powerhouse), 1/10,000 (Waterway), 1/25,000 (Reservoir area)

b. Investigation Drillings (Details are shown in **Table 7.2.1-1**)

Area of Survey : Dam site, Outlet of Diversion Tunnel, Powerhouse & Surge tank (Previous plan)

Quantity : 7 holes 312.8 m

c. Seismic prospecting

Area of Survey : Dam site, Powerhouse site (Previous plan)

Quantity : 26 survey lines, 3,335 m

d. Investigation for the construction materials

Test pits: : 27 pits

Table 7.2.1-1 Investigation Drillings carried out by NEA on 2000

Drill hole No.	Length (m)	Elevation (m)	Inclination & Direction		Location	Co-ordinate		Remarks
			Inclination	Direction				
DDH-1	50.0	308.6	90°	*	Dam axis, R/B	525464.41	3092810.39	
DDH-2	7.0	309.2	70°	N280	Downstream of dam axis (L/B)	525444.1	3092882.24	
	8.5	309.2	65°	N280	ditto			
	8.8	309.2	60°	N280	ditto			
	12.0	309.2	90°	*	ditto			
	11.0	309.2	45°	N280	ditto			
DDH-3	50.0	318.2	75°	N312	Downstream of dam axis (L/B)	525500.19	3092993.88	
DT-2	25.0	323.2	60°	N165	Diversin Outlet	525623.88	3092955.64	
DPH-1	50.0	328.9	90°	*	Powerhouse	527423.68	3092468.98	Old Layout
DPH-2	24.5	299.6	75°	N270	Alternative Powerhouse	527833.34	3092772.4	Old Layout
DST-1	66.0	472.2	90°	*	Surgetank	527168.13	3092494.15	Old Layout
Total	7 holes	312.8 m						

7.2.2 Geological Investigation Works carried out in the Study

The geological investigation works carried out in the Study are as follows;

a. Geological Reconnaissance

Area of Survey : Dam site, Powerhouse site, route of waterway and reservoir area

Scale of the map used : 1/1,000 (Dam, Powerhouse and outlet of Tailrace),
1/25,000 (Reservoir area)

b. Investigation Drillings (Details are shown in **Table 7.2.2-1**)

Area of Survey : Dam site, Outlet of Diversion and tailrace, Powerhouse & Intake

Quantity : 19 holes 1,623.3 m

Permeability Tests : 194 test sections

c. Laboratory Test of the drilled core

Sampling Location : Damsite, Intake, Outlet of Tailrace

Quantity : Uniaxial Compression Tests;28 samples, Tensile Strength Tests;15 samples, Physical Property tests (Specific Gravity and absorption);22 samples

Table 7.2.2-1 Investigation Drillings carried out in the Study

Drill hole No.	Length (m)	Elevation (m)	Inclination & Direction		Location	Coordinate		Remarks
			Inclination	Direction		E	N	
B-1	150.0	515.00	90°	*	Dam axis, L/B	525,298.850	3,092,828.490	by NEA
B-2	100.0	408.00	45°	N287	Dam axis, L/B	525,389.560	3,092,788.590	ditto
B-3	100.55	328.50	45°	N287	Dam axis, L/B	525,417.220	3,092,706.400	ditto
B-4	120.5	328.50	80°	N287	Dam axis, L/B	525,417.220	3,092,706.400	ditto
B-5	100.5	307.93	90°	*	Dam axis, River bed	525,459.840	3,092,798.930	ditto
B-6	92.0	307.93	45°	N107	Dam axis, River bed	525,459.840	3,092,798.930	ditto
B-7	50.0	307.93	45°	N287	Dam axis, River bed	525,459.840	3,092,798.930	ditto
B-8	100.0	401.60	45°	N107	Dam axis, R/B	525,502.470	3,092,723.720	ditto
B-9	150.0	527.50	90°	*	Dam axis, R/B	525,590.680	3,092,749.380	ditto
B-10	30.0	308.45	90°	*	Dam toe, R/B	525,487.210	3,092,868.890	ditto
B-11	30.0	307.46	90°	*	Dam toe, L/B	525,445.510	3,092,875.740	ditto
B-12	120.0	401.60	45°	N020	Dam axis, R/B	525,502.470	3,092,723.720	ditto
BP-1	100.0	370.97	50°	N180	Underground Powerhouse (Option2)	525,622.522	3,092,888.654	ditto
BH-1	90.0	430.95	90°	*	Intake (Option 2)	525,567.697	3,092,659.422	by Study team
BH-2	50.0	320.09	90°	*	Diversion Outlet	525,737.629	3,092,966.836	ditto
BH-3	50.0	331.79	90°	*	Tailrace Outlet (Option2)	525,634.116	3,092,947.201	ditto
BH-4	90.0	427.02	90°	*	Intake (Option 3)	525,669.118	3,092,472.343	ditto
BH-5	50.0	358.31	90°	*	Downstream of dam (L/B)	525,591.511	3,093,103.786	ditto
BH-6	50.0	313.60	90°	*	Tailrace Outlet (Option 3)	527,052.143	3,092,078.266	ditto
Total	19 holes	1623.55 m						

< Note> Three investigation drillings for the Option III-b underground powerhouse are planned. They are commenced on March, 2007 by NEA and are under drilling on June 2007.

7.3 Site Geology

7.3.1 Reservoir

(1) Topography

The Seti River, which originates in the Annapuruna mountain range, runs through the Pokhara valley. The river flows in N-S direction around the upstream end of the reservoir; it turns the direction abruptly and flows straight in E-W direction to the dam site. The Seti River changes the flow direction again from E-W to N-S near the dam site, and it interflows with the Madi River at approximately 2 km downstream of the dam site. Passing the confluence, it takes curve and flows in south to SWS direction. The rugged mountain land of which elevation is about 1,000 m spread in E-W direction in the left bank and the middle to upstream of the right bank of the reservoir. On the other hand, the mountain in the upper stream area of the right bank of the reservoir forms rather smooth slope of 700 to 800 m above sea level.

The length of the reservoir is approximately 18 km. The reservoir from the dam site to 11 km upstream of the dam site forms a steep valley; the inclination of the slope of both banks of the reservoir is about 40 degree in this area. The upstream area of the reservoir shows the relatively gentle topography with several terrace plains in both banks, especially in the right bank, and several tributaries from south or southwest. The wide spread terrace plain from Jaruwapani to Bhimad Bazzar, near the upstream end of the reservoir, on the right bank of the reservoir is utilized as cultivated field, and villages are scattered on it. The terrace deposit forms the vertical cliffs of 20 to 30 m in height in many places because of the erosion by the Seti River, and the houses or cultivation field are distributed on the top of cliffs.

The width of the valley at the full supply level (FSL), EL.415 m, is about 90 m at the dam axis, 300 m to 400 m from the dam site to 11 km upstream of the dam site, and 500 m to 600 m in the upstream area of the reservoir.

Large landslide, collapse landform and the narrow saddle adjacent to the other drainage basin are not observed in the reservoir area.

(2) Geology

Reservoir area is composed of Pre-Cambrian to Paleozoic dolomite, slate, phyllite and Quaternary deposit of terrace deposit, talus deposit and recent river deposit as shown in **Fig.7.3.1-1**.

Dolomite is distributed in the left bank from the dam site to the middle part of the reservoir with the strike of E-W, parallel to the Seti River, and dip of 40 to 60 degree to south. Although the solution cavities of several cm to several 10 cm in diameters are observed at

the dam site in some places, the prominent karst phenomenon or karst topography is not confirmed in the reservoir area as the result of the field investigation and the aerial-photo interpretation. Slate and phyllite are distributed in the right bank from the just upstream of the dam site to the middle part of the reservoir and in the both banks of the upstream area. They strike E-W and dip 40-60 to south in the same direction as the dolomite. The boundary between dolomite and slate/phyllite is presumed to be a fault which runs from the 200 m upstream of the dam site to Tuttuwa along the Seti River.

Most of the talus deposit is distributed in the area lower than the high water level, EL.415 m except for the several places in the middle to upstream area of the reservoir. Terrace deposit is found in the area from Geruwa, which is located in the upstream area, to Bhimad Bazaar near the upstream end of the reservoir. According to the aerial-photo interpretation, 6 different terrace plains are recognized. The elevation of the terrace plain at Geruwa is about EL.380 m and the elevation of the plain at Bhimad Bajar ranges from EL.440 m to 460 m. These terrace deposits are composed of pebble to cobble of slate and limestone with calcareous silt to fine grained sand matrix. Characteristics of the terrace deposits vary from place to place in some degree; the deposit in some places consists of silt and fine sand with thin layer of pebble and cobble, and the deposits in other places are composed mainly of pebble and cobble. The terrace deposit in this area belongs to Pokhara formation named by Yamanaka et. al. (1982). Yamanaka et al. (1982) divided the deposits of the Pokhara valley into nine stratigraphic units based on the unconformities and their lithofacies. They described the general characteristics of the Pokhara formation as follows;

“The Pokhara Formation consists of fluvial gravel deposited by Seti River and of pebble and cobble sized, sub-angular to sub-rounded and ill-sorted gravel mainly of limestone and calcareous shale along with small quantity of gneiss, granite and schist. These gravels are filled with matrix of grey or light brown calcareous silt or fine sand. The Pokhara Formation has been characterized by its low degree of cementation.”

Hormann (1974) had considered that the Pokhara formation was accumulated during the last glacial age but Yamanaka et. al., (1982) and M. Fort (1987) had performed radiocarbon dating for the Pokhara Formation. Yamanaka et. al., (1982) have determined the age of the Pokhara Formation is 590 year B.P. to 1070 years B.P. (Before Present) while M. Fort (1987) has determined the age of the Formation is 400 years B.P. to 1100 years B.P. These findings indicate that the Pokhara Formation belongs to the Holocene Age, i.e. the post-glacial age.

(3) Geotechnical Evaluation

1) Watertightness of the reservoir

- Slate and phyllite are widely distributed in the reservoir area. Generally, the high permeability zone does not continue through these types of rocks except for the surface weathered zone and fault zone. Furthermore, the flowing water is observed in the small stream in the mountain of slate and phyllite. This suggests that the groundwater is high in the area composed of slate and phyllite.
- Dolomite is distributed in the left bank of the lower reach and middle part of the reservoir. However, the prominent karst topography is not confirmed in dolomite of the reservoir area, and slate and phyllite are found in the large area north of the dolomite distributed area.
- The narrow saddle or thin ridge, which has the possibility of the leakage to the adjacent drainage basin, is not observed in the reservoir area.
- Judging from the topographic and the geologic condition mentioned above, it is considered that the watertightness of the reservoir is assured.

2) Stability of the slope

The geological phenomenon concerned to the slope stability around the reservoir is the landslide, thick talus deposit and the terrace deposit which forms the vertical cliff at the upstream area.

a) Landslide and talus deposit

- Small landform of old landslides and slope failures are observed in some places. However, they are located in the area of EL.500 m to 700 m, higher than FSL of EL.415 m; they have no effect on the reservoir.
- Some of talus deposits are distributed from the riverbed to the area higher than the high water level. Considering the small scale of those talus deposits, they do not cause damage to the reservoir and surrounding environment even if a part of those deposits are collapsed.

b) Terrace deposit

- The terrace deposits form the vertical cliffs in many places from Geruwa to Bhimad Bazaar because of the erosion by the Seti River. These cliffs are not completely stable under the present situation. It is presumed that the cliffs will be collapsed progressively and they will move toward the mountainside keeping their vertical shape. For example, phenomenon, which shows the instability of the cliff, is observed at the cliff of about 25 m in height in Bhimad Bajar. At this cliff, several surface collapses of 3 m in height are observed at the bottom of the cliff

and the fissures parallel to cliff are found in the middle portion of the cliff. These surface collapses and fissures are assumed to be caused by the erosion or the strength reduction of the deposit by the infiltration of the river water during the flood season. The similar cliffs of the terrace are found in many places from Bhimad Bajar to Jaruwapan about 6 km downstream. The countermeasure or mitigation against the erosion is necessary for these cliffs. The details of the method and the extent of them should be examined based on the detailed topographic map and geologic map scale of 1/1,000 to 1/5,000 during the detailed design stage.

7.3.2 Dam

(1) Topography

The dam site is located in the Seti River about 2 km upstream of the confluence of the Seti River and the Madi River. The elevation of the riverbed at the dam axis is about EL.300 m. The Seti River flows in E-W direction from the upstream end of the reservoir. It changes the direction to north at the point about 200 m upstream of the dam axis, and it turns to east again at the 200 m downstream of the dam axis.

The right bank of the dam is composed of the narrow ridge of EL.500 m to 550 m which extends in E-W direction. It is a branch of the main ridge of EL.500 m to 1,000 m stretching in N-S direction. The width of the right bank ridge at FSL, EL.415 m, is 150 m to 200 m. The left bank of the dam is located at the east end of the ridge of EL.1,000 m which extends along the left bank of the reservoir.

The inclination of the right bank slope is about 75 degree from the riverbed to EL.380 m, and 60 degree above EL.380 m. The inclination of the left bank slope is 70 to 80 degree from the riverbed to EL.410 m, and 45 degree above EL.410 m. No topsoil is distributed on both banks except for a part of the left bank slope above EL.410 m. The rock outcrops on both riverbanks extend for more than 200 m in upstream and about 100 m in downstream of the dam axis. The width of the river is about 30 m and the width of the valley at FSL, EL.415 m, is about 90 m at the dam axis.

(2) Geology

Late Pre-Cambrian to early Paleozoic dolomite, Dhading Dolomite, and talus deposit, recent river deposit are distributed in the dam site as shown in **Fig.7.3.2-1** and **Fig.7.3.2-2**.

1) Foundation Rocks

Dam foundation is composed of grey to dark grey dolomite. The dolomite is hard and thick bedded in general, but the phyllitic dolomite layers of 1 to 2 m thickness, which

tends to fine fragments, are intercalated in some places. Quartzite and dolomitic quartzite of 3 to 4 m in thickness are found in the dolomite in HB-1 drilled at the Intake site. These layers strike WNW-ESE to E-W and dip 45 to 60 degree to south, namely they cross the river at rights and incline to upstream side. Weathering degree of the foundation rocks is low in general; the weathered zone of 1 to 5 m in thickness, which shows the brown color caused by oxidation, is found only in the high portion of both banks.

Solution cavities of several cm to several 10 cm in diameter are found in the dolomite in places at dam site. Prominent solution cavities are observed at the area near the top, EL.530 m, of the right bank ridge. Maximum diameter of the solution cavities at this area is approximately 1 m. However, the drillhole B-9 drilled at the area shows that the solutions along the joints are observed from the surface to 20 m depth, EL.507 m, but no solution phenomenon is found in deeper than 20 m depth. On the left bank, solution cavities of several cm to 20 cm are observed along the joint plane and small fault in places on the path of EL.330 m. Further, the solution cavity of 60 cm in diameter is found in the drillhole B-1 at the depth of 138 m, EL.377.1 m, and slightly solutions along the joints are confirmed from 3 to 5 m in depth, EL.304 to 306 m, of DDH-2 which is drilled at near the riverbed downstream of dam axis. Among of the 15 drillholes at the dam site of which total length is 1,290 m, the solution phenomenon is observed only in three sections of 138 m depth of B-1, 4 to 20 m depth of B-9 and 3 to 5 m depth of DDH-2.

Large fault is not confirmed in the dam site, but several small faults of 20 to 200 cm in width are found in places. These small faults have a few fault clay and form highly jointed zone of which joint spacing is 1 to 2 cm. These faults strike N-S to NW-SE, and dip 20 to 30 degree to southwest. The phyllitic dolomite layers are generally jointed, and show the condition similar to fault zone.

Main joint system at the dam site is a) WNW-ESE, 40-50S, b) N-S, 80-90E, c) NW-SE, 50SW, d) NE-SW, 80-90N.

2) Surface deposit

a) Talus deposit

On the right bank, thick talus deposit is distributed in the northern slope of the right bank ridge about 100 m to 400 m downstream of the dam axis. On the left bank, thin talus deposit is distributed in the relatively gentle slope, 40 degree inclination, above EL.410 m.

b) Recent river deposit

The thickness of the recent river deposit is 15 m at the Drillhole B-10, and 18 m at the drillhole B-11 which are drilled at the riverbed 50 m downstream of the dam axis.

The inclined drillhole B-7 of which inclination is 45 degree at the dam axis shows the 18 m thickness of the river deposit.

3) Rock mass classification

Rock mass classification is carried out based on the three factors of weathering, hardness and joint spacing. The rock mass condition is evaluated by the combination of these three factors. Standard of the rock mass classification and rock mass evaluation are shown in **Table 7.3.2-1** and **Table 7.3.2-2**.

Table 7.3.2-1 Standard of Rock Mass Classification (for Drilled Core)

CLASS	WEATHERING	HARDNESS	JOINT SPACING
1	Very fresh. No weathering of mineral component.	Very hard. Broken into knife-edged pieces by strong hammer blow.	over 30 cm
2	Fresh. Some minerals are weathered slightly. Usually, no brown crack.	Hard. Broken into pieces by strong hammer blow.	10 to 30 cm
3	Fairly fresh. Some minerals are weathered. Cracks are stained and with weathered mineral.	Brittle. Broken into pieces by medium hammer blow.	5 to 10 cm
4	Weathered. Fresh portions still remain partially.	Very brittle. Easily broken into pieces by slight hammer blow.	1 to 5 cm
5	Strongly weathered. Most of minerals are weathered and altered to secondary minerals.	Soft. Able to dig with hammer.	under 1 cm

Table 7.3.2-2 Standard of Rock Mass Evaluation

		Joint Spacing								
Weathering	Hardness	1	1~2	2	2~3	3	3~4	4	4~5	5
1	1	A								
	1~2		B							
2	2				CH					
	2~3									
3	3						CM			
	3~4									
4	4								CL	
	4~5									D
5	5									

a) Right bank of the dam

As the result of the B-9 hole drilled at the upper portion of the right bank, the rock mass condition is as follows;

- From the ground surface to 42 m depth; Good rock condition of CH class, RQD ranges from 0 to 74%, average RQD of this section is 34%.
- From 42 m to 105 m depth; CM class and CM~CL class, RQD ranges from 0 to 44%, average RQD of this section is 6%.
- From 105 m to 150 m depth; Highly jointed rock of CL class, RQD ranges from 0 to 37%, average RQD of this section is 4%.

As the result of the B-8 hole drilled at the middle portion of the right bank, the rock mass condition is as follows;

- From the ground surface to 33 m depth; Highly jointed rock of CM~CL class and CL class, RQD ranges from 0 to 26%, average RQD of this section is 2%.
- From 33 m to 91 m depth; CM class and CH class, RQD ranges from 0 to 49%, average RQD of this section is 12%.
- From 91 m to 100 m depth; Highly jointed rock of CM~CL class and CL class, RQD is 0%.

As the result of the B-12 hole drilled at the middle portion of the right bank, the foundation rock consists of the jointed rock of CM~CL class and relatively good rock of CM~CH class which are observed repeatedly until the bottom of the hole. RQD of the B-12 ranges from 0 to 67%, and average RQD is 9%.

As the result of the B-6 hole drilled at the lower portion of the right bank, the rock mass condition is as follows;

- From the ground surface to 74 m depth; Good rock mainly of CH class, RQD ranges from 0 to 82%, average RQD of this section is 32%.
- From 74 m to 91 m depth; CM~CL class and CM class, RQD ranges from 0 to 22%, average RQD of this section is 5%.

b) Riverbed

As the results of the B-5 and B-7 holes, the riverbed consists of relatively good rock of CH class, CM class and CH-B class in parts. RQD of the B-5 ranges from 0 to 78%, and average RQD is 15%, and RQD of the B-7 ranges from 0 to 78%, and average RQD is 21%.

c) Left bank of the dam

As the result of the B-1 hole drilled at the upper portion of the left bank, the rock mass is composed of good rock of CH class except for the section from 138.0 m to 144 m.

The section from 138.0 m to 144.0 m is jointed rock mass of CL class. RQD of the B-1 ranges from 0 to 89%, and average RQD is 33%.

As the result of the B-2 hole drilled at the middle portion of the left bank, the rock mass condition is as follows;

- From the ground surface to 6.4 m depth; Jointed rock of CM~CL class.
- From 6.4 m to 65 m depth; Very good rock mainly of B class. RQD ranges from 0 to 93%, average RQD of this section is 59%.
- From 65 m to 100 m depth; Relatively good rock of CH class and CH~CM class, RQD ranges from 0 to 69%, average RQD of this section is 30%.

As the result of the B-3 and B-4 holes drilled at the lower portion of the left bank, the rock mass is composed of relatively good rock of CH class and CM class. RQD of the B-3 ranges from 0 to 89%, and average RQD is 35%, and RQD of the B-4 ranges from 0 to 88%, and average RQD is 42%.

4) Groundwater

a) Right bank of the dam

Groundwater is not found in the drillholes of B-8, B-9 and B-12 on the right bank. However, the groundwater is confirmed at 56 m depth, EL.328.7 m, of the BP-1 inclined hole which is excavated from the downstream slope of the dam to the underground powerhouse site for Option II layout. Further, the groundwater is confirmed at 81 m depth, EL.350.7 m, of the BH-1 which is drilled at the Intake site upstream of dam axis. These data shows that the groundwater level in the right bank is rising up toward the mountain side even though the water level is low.

b) Left bank of the dam

Among 4 drillholes excavated in the left bank, the groundwater is found at 21 m depth, EL.313.65 m, of the B-3 hole and 20 m depth, EL.308.8 m, of the B-4 hole. These B-3 and B-4 holes are drilled at the lower portion of the slope. The groundwater is not found in the B-2 hole drilled at the middle portion of the slope. In the B-1 hole at the upper portion of the slope, the groundwater is not found in the dry season, but it is observed from 139 m to 144 m depth, EL.377.1 m to 376.1 m, in rainy season.

5) Permeability

Permeability test results carried out at the damsite are shown in **Table 7.3.2-3**.

Table 7.3.2-3 Results of the Lugeon Tests at the Damsite

Left Bank								River Bed						Right Bank					
B-1		B-2		B-3		B-4		B-5		B-6		B-7		B-8		B-9		B-12	
Depth(m)	Lu	Depth(m)	Lu	Depth(m)	Lu	Depth(m)	Lu	Depth(m)	Lu	Depth(m)	Lu	Depth(m)	Lu	Depth(m)	Lu	Depth(m)	Lu	Depth(m)	Lu
0-5	NT	0-5	NT	0-5	NT	0-5	NT	0-5	NT	0-5	NT	0-5	NT	0-5	NT	0-5	NT	0-5	NT
5-10	NT	5-10	NT	5-10	NT	5-10	NT	5-10	NT	5-10	NT	5-10	NT	5-10	NT	5-10	NT	5-10	NT
10-15	1.35	10-15	53.0	9.85-14.85	35.86	10.8-14	12	10-15	NT	10-15	1.8	10-15	NT	10-15	NT	10-15	NT	10-15	NT
15-20	8.8	15-20	65.0	14.95-19.95	34.56	15.3-18.5	30.82	15-20	NT	15-20	1.2	15-20	NT	15-20	NT	15-20	NT	15-20	13.3
						18.3-21.5	44.3												
20-25	NT	20-25	63.0	20-25	4.49	22.8-26	36.74	22.5-25.5	3.4	20-25	10.0	20-25	NT	20-25	9.11	20-25	29.0	20-25	NT
25-30	2.7	25-30	55.0	25-30	3.19	26.0-30.3	NT	25.5-28.5	2.68	25-30	1.40	25-30	NT	25-30	11.0	25-30	31.0	24.4-29.4	52.0
								28.5-31.5	4.14										
30-35	1.7	30-35	34.0	30-35	4.53	30.3-33.5	43.8	31.5-34.5	1.37	30-35	27.0	30-35	7.75	30-35	NT	30-35	28.0	30-35	NT
35-40	NT	35-40	38	35.6-40.6	5.33	37.8-41	2.00	34.5-39	1.86	35-40	1.48	35-40	3.10	35-40	31.8	35-40	18.0	35-40	0.13
40-45	23.9	40-45	26.0	40.5-45.5	15.09	41-44.2	2.57	39-43.5	2.93	40-45	1.30	40-45	1.70	40-45	NT	40-45	22.0	40-45	5.18
45-50	NT	45-50	17.0	45-50	NT	44.05-47.25	6.45	43.5-48	3.08	45-50	2.10	45-50	2.15	45-50	1.23	45-50	25.0	45-50	1.0
						47.2-50.4	1.57												
50-55	16.21	50-55	15.0	51.3-56.3	2.11	51.3-54.5	2.45	48.15-54.15	4.33	50-55	1.60			50-55	5.02	50-55	15.0	50-55	NT
55-60	2.23	55-60	14.0	56.75-61.75	2.71	55.8-59	1.64	54.15-58.65	4.61	55-60	1.0			55-60	2.88	55-60	14.0	54-59	1.92
60-65	1.17	60-65	13.0	60-65	NT	59.8-63	1.82	58.65-63.15	1.46	60-65	1.40			60-65	1.21	60-64.95	12.0	60-65	NT
						63.4-66.6	5.22												
65-70	1.0	65-70	18.0	64-69	2.50	67.97-71.17	2.38	63.15-67.65	0.90	65-70	2.90			65-70	NT	65-70	NT	65-70	0.61
70-75	1.7	70-75	5.0	69.9-74.9	2.00	72.3-77.3	1.05	67.65-72.15	1.26	70-75	2.35			70-75	18.0	70-75	NT	70-75	NT
								72.15-76.65	0.93										
75-80	1.49	75-80	6.0	75.05-80.05	1.79	77.4-82.4	1.27	76.65-81.15	13.7	75-80	NT			75-80	4.5	77-82	2.0	73.35-80.35	1.36
80-85	1.67	80-85	NT	80.2-85.2	2.10	82.65-87.65	2.00	81.15-85.65	0.46	80-81.2	1.38			80-85	18.3	80-85	NT	80.65-85.65	3.86
85-90	1.04	85-90	7.0	85-90	1.50	88.6-93.6	1.30	85-90	NT					85-90	6.49	85-90	NT	85-90	NT
90-95	11.7	90-95	9.0	90-95	NT	93.7-98.7	1.95	90-95	NT					90-95	22.4	90-95	NT	91.3-96.3	3.86
95-100	0.57	95-100	10.0	95.5-100.5	2.55			96-100.5	0.88										
100-105	NT					99.1-104.1	1.42									100-105	NT	100-105	1.72
105.8-110.8	4.49					104.3-109.3	2.09									104-109	6.0	105-110	12.6
110-115	NT					110-115	NT									110.2-115.2	10	110-115	NT
115-120	1.76					115.5-120.5	3.39									115-120	NT	115-120	5.08
120-125	NT															120-125	NT		
125-130	0.84															125-130	NT		
130-135	NT															129-134	7.0		
135-140	NT															135-140	NT		
140-145	NT															140-145	NT		
145-150	1.6															145-150	5.0		

Remarks: NT stands for No Lugeon Test

a) Right bank of the dam

As the results of the Lugeon tests in the B-9 hole at the upper portion of the slope, the permeability of the foundation rock from the ground surface to 65 m depth is high of $Lu=10\sim30$, and the permeability from the 65 m to 150 m is rather low of $Lu=5\sim10$. However, the section where Lugeon tests are executed is only 40% of the total length of the hole because of the highly jointed condition of the hole. As the results of the Lugeon tests in the B-8 and B-9 holes at the middle portion of the slope, the permeability of the foundation rock from the ground surface to 30~40 m depth is high of $Lu=10\sim50$, and the permeability below that depth is low of $Lu=1\sim3$ in general. However, there are some places with high permeability in deep portion such as the section of 70~100 m of the B-8 hole where the Lugeon value is $Lu=10\sim20$. As the results of the Lugeon tests of the B-6 hole at the lower portion of the slope, the permeability is low of $Lu=1\sim3$ in general, but some paces shallower than 35 m shows $Lu>10$.

b) Riverbed

Permeability of the foundation rock is low of $Lu=1\sim4$ in the B-5 hole (test section is 22.5~100 m) and the B-7 hole (test section is 30.0~50.0 m). Lugeon test results in DDH-1, which is drilled at the riverbed 15 m downstream of the B-5, shows high permeability of $Lu>50$ from the ground surface to 27.7 m depth, and low permeability of $Lu=1\sim4$ in the area deeper than 32 m.. Therefore, the section from 0 to 22.5 m of the BH-5 hole where the Lugeon test is not carried out is presumed to be high permeability.

c) Left bank of the dam

As the results of the Lugeon tests in the B-1 hole at the upper portion of the slope, the permeability of the foundation rock is low of $Lu=1\sim2$ except for the section from 20 m to 55 m depth where the permeability is high of $Lu=15\sim30$. However, Lugeon tests are carried out in only 40% section of the total length of the hole deeper than 100 m, the portion around 138 m depth, where the solution cavity of 60 cm diameter is found, should be highly permeable. As the results of the Lugeon tests in the B-2 hole at the middle portion of the slope, the permeability of the foundation rock is high of $Lu=13\sim65$ from the ground surface to 70 m depth, and the permeability is relatively low of $Lu=5\sim10$ at the section deeper than 70 m depth. As the results of the Lugeon tests in the B-3 hole and B-4 hole at the lower portion of the slope, the permeability of the foundation rock from the ground surface to 25~35 m depth is high of $Lu=30\sim40$, and that is low of $Lu=1\sim5$ deeper than 35 m depth.

(3) Geotechnical Evaluation

Judging from the surface geological condition and the results of the investigation drillings including permeability tests, the dam site is evaluated from the view point of engineering geology as follows;

- 1) The dam site is composed of the Pre-Cambrian to Paleozoic dolomite. The dolomite is hard and fresh in general, but the highly jointed layers and small faults are distributed in places. According to the results of the investigation drillings, the left abutment of the dam is composed of the good rock of CH class and B class, and the riverbed consist of the relatively good rock of CH class and CH~CM class in parts. On the other hand, the right abutment consists of the jointed rock in general except for the lower portion near the riverbed. The investigation drillings at the right bank are comprised of fragmental core or core loss portion in many sections. However, as the result of the B-12 hole, which is drilled at 15 m lower than FSL, the relatively good rock of CH~CM class is distributed in the portion deeper than 30 m from the ground surface.

Considering the above mentioned geological condition, the foundation rock of the dam site is judged to have a sufficient bearing capacity for the foundation of the concrete gravity dam of 140 m in height. However, the rock condition of the right abutment should be confirmed by the exploratory adit, and the deformability characteristics and the strength of the foundation rocks should be clarified by the in-situ tests in the adit at D/D stage.

- 2) As the result of Lugeon test at the dam site, the high permeability zone of $Lu > 10$ is the portion from the ground surface to 70 m depth in the left bank and the portion from the ground surface to 40 m depth in the right bank. The area deeper than those depth shows low permeability of $Lu = 2 \sim 10$ or $Lu < 2$ except for a part of the right bank. The deep high permeability zones in both banks are estimated to be caused by the relaxation along the joints in steep slopes.

Considering the followings, the permeability of the foundation rock in the dam site is presumed to be controlled by the discontinuity planes such as joints, and the solution cavities seems to have a little effect on the permeability of the foundation rocks.

- The permeability of the foundation rocks get lower progressively as the depth.
 - The groundwater level is rising up toward the mountain side in both banks even though the water level is low.
 - The solution cavities observed in the drilled core of which total length is 1,290 m at the dam site, is very few.
- 3) The permeability of the foundation rocks and the groundwater level should be clarified to examine the foundation treatment, the depth and the extent of the grouting. Although it is confirmed that the groundwater level is rising up toward the mountain side in both banks,

the groundwater level is located in the deep portion of both banks, which is 70 m lower than FSL. Accordingly, the groundwater level in the mountain of the both banks should be investigated at D/D stage. Drillings from the adit mentioned in a) or from the ground surface for the investigation of the groundwater level are recommended.

- 4) Thick talus deposit and landslide, which have a disadvantage for the dam excavation, are not distributed in the dam site.

7.3.3 Waterway and Powerhouse (Option-II)

(1) Topography

The intake, the underground powerhouse and the outlet of tailrace of the option-II are located in the right bank ridge which extends in E-W direction. The length of the headrace tunnel and the tailrace tunnel are 170 m and 100 m respectively, and the maximum rock cover of the tunnel is about 230 m. The underground powerhouse is located in the northern part of the ridge, so the rock cover is about 90 m in vertical and about 50 m from the northern slope of the ridge. The intake is located in the southern slope of the ridge of which inclination is about 50 degree. The outlet of tailrace is situated in the northern slope of the ridge. The inclination of the slope above EL.390 m is steep, 55 to 65 degree, and the slope below EL.390 m forms gentle slope of 30 to 40 degree inclination because of the thick talus deposit.

(2) Geology

The waterway and the underground powerhouse are composed of dolomite as shown in **Fig.7.3.2-1** and **Fig.7.3.3-1**. The river deposit and the thick talus deposit cover the dolomite at the outlet of tailrace.

1) Waterway and Underground powerhouse

As the result of the drill hole BP-1, the underground powerhouse consists of jointed dolomite in general. The foundation rock from 10 m to 77 m depth is composed mainly of CM class intercalating CH class and CL class, and the foundation rock deeper than 77 m consists of highly jointed rock of CL class. RQD of the section between 10 m to 75 m ranges from 0 to 47%, of which average is 7%, and RQD of the section between 75 m to 100 m ranges from 0 to 13%, of which average is 1%.

As the result of the Lugeon test of BP-1 hole, the permeability of the foundation rock is high of $Lu=10\sim30$ in the section from 10 m to 52 m. The permeability decreases as the depth, Lugeon value between 52 m to 70 m is $Lu=3\sim6$ and the Lugeon value between 70 m to 100 m is less than $Lu=2$. Groundwater level is confirmed at 56 m depth, EL.328.07 m.

The waterway is composed of dolomite. Judging from the results of BH-1, BP-1 and B-9, the rock condition of the waterway route is presumed to be jointed in general though a large fault is not estimated in this area.

2) Intake

The slope where the intake is located consists of dolomite without prominent surface deposit. As the result of the drill hole BH-1 at the intake site, the foundation rock from the ground surface to 39 m depth is relatively good rock of CH class, and the foundation rock below the 39 m depth is highly jointed rock of CM~CL class and CL class. RQD of the section between 3 m to 39 m ranges from 0 to 88%, of which average is 32%, and RQD of the section between 39 m to 90 m ranges from 0 to 31%, of which average is 4%. The permeability of the foundation rock is high of $Lu=28\sim90$ in the section from 15 m to 45 m, it is low of $Lu=0.5\sim3.0$ in the section deeper than 55 m.

3) Outlet of Tailrace

Dolomite, river deposit and talus deposit are distributed in the outlet of tailrace. Talus deposit is thickly distributed in the northern slope of the right bank ridge. The thickness of the talus deposit is about 30 m in the BH-3 hole at the outlet site and is about 10 m in the BP-1 hole which drilled at the site about 40 m upper than BH-3 hole. The boundary between the talus deposit and river deposit is confirmed at 39.9 m depth, EL.291.9 m.

(3) Geotechnical Evaluation

- 1) The arch of the underground powerhouse is situated at the 60 m depth of the BP-1 drillhole. As the result of the BP-1 hole, the foundation rock from 10 m to 77 m depth consists of the relatively jointed rock of CM class, and the foundation rock deeper than 77 m depth, which corresponds to the lower portion of the powerhouse cavern, is composed of highly jointed rock of CL class. RQD of the foundation rock between 50 m to 65 m corresponding to the arch of the powerhouse cavern ranges from 0 to 47% and 18% in average.
- 2) The rock mass of the underground powerhouse is classified to “Very poor rock” to “Poor rock” of the RQD classification of Deer, 1967. According to the RMR (Rock Mass Rating) classification of Bieniawski, 1989, the foundation rock of the arch portion is evaluated as “Fair rock” of $RMR=43\sim48$, and the foundation rock of the lower portion of the cavern is evaluated as “Poor rock” of $RMR=27\sim37$ as shown in Table 7.3.3-1.
- 3) The rock evaluation mentioned above is based on the result of only one drill hole of the BP-1. As the distribution of the jointed zone of CL class is not clear now, it may appear at the arch portion of the cavern.

- 4) Volume of the inflow of the groundwater during the cavern excavation is estimated to be few, because the groundwater level is low, 5 m above the arch, and the permeability of the foundation rock is low as the result of the BP-1 hole.
- 5) As the result of the BH-1 hole at the intake site, the foundation rock from the ground surface to 39 m depth consists of good rock of CH class. It is judged that the intake shaft will be excavated without big trouble. Thick talus deposit and the landslide are not found in the slope where the intake is planned.
- 6) Thick talus deposit and the river deposit are distributed in the outlet of tailrace site, and the basement of the outlet is located in the river deposit. The excavated slope of which height is about 20 m consists of talus deposit.

Table 7.3.3-1 RMR of the Underground Powerhouse of Option-II

Strength of intact rock material	Arch		Lower portion of Cavern	
	50-100 Mpa	50-100 Mpa	25 – 50 Mpa	25 – 50 Mpa
Rating	7	7	4	4
RQD	< 25%	< 25%	< 25%	< 25%
Rating	3	3	3	3
Spacing of discontinuities	6 – 20 cm	6 – 20 cm	< 6 cm	< 6 cm
Rating	8	8	5	5
Condition of discontinuities	S.R & S.W.	S.R & S.W.	S.R & H.W.	S.R & H.W to Slickesided
Rating	25	25	20	15
Groundwater condition	Damp	Damp	Damp	Damp
Rating	10	10	10	10
Discontinuity orientation	Fair	Unfavourable	Fair	Unfavourable
Rating	- 5	-10	- 5	- 10
RMR	48	43	37	27

< Note> S.R; Slightly Rough, S.W.; Slightly Weathered, H.W.; Highly Weathered

7.3.4 Waterway and Powerhouse (Option-III b)

(1) Topography

In the plan of the option-III b, the intake is located in the right bank slope about 400 m upstream of the dam axis, and the waterway 1.5 km long will be excavated from the intake site in WNW-ESE direction. The Seti River flows to north at the dam site but changes the flow direction to south at the confluence of Seti River and Madi River. The outlet of tailrace is located at the Seti River, which runs to south, about 5 km downstream of the dam axis. The waterway tunnel crosses the ridge of EL.600 m~1,000 m, which extends from south to north. The rock cover of the waterway tunnel is 200~650 m and that of the underground powerhouse is 300~400 m.

(2) Geology

1) Waterway and Underground powerhouse

Phyllite including salty phyllite is distributed in the upstream area of the tunnel route and dolomite in the downstream area as shown in **Fig.7.3.4-1**, **Fig.7.3.3-2** and **Fig.7.3.4-3**. The 700 m section from the intake is composed of phyllite and slaty phyllite, and dolomite is distributed in the underground powerhouse site and the 60% of the waterway tunnel route including the penstock and the outlet of tailrace.

Phyllite, and dolomite strike E-W to NW-SE and dip 45-50S to 45-50SW, namely they are nearly parallel to the axis of the tunnel.

2) Intake

Phyllite and slaty phyllite are distributed in the intake site. As the result of the BH-4 hole, the foundation rock from the ground surface to 35 m depth is composed of jointed rock. Especially, the section between from 15 m to 35 m is highly jointed, and the drilled cores are composed of few small fragments in this section. The permeability of the foundation rock is low of $Lu=2\sim 8$, and the groundwater is confirmed at 18.7 m depth, EL.408.3 m. The slope where the intake is planned is relatively gentle, the inclination is about 40 degree, but the thick talus deposit and landslide are not found in this area.

3) Outlet of tailrace

The outlet of tailrace is located at the east side of the dolomite cliff, and consists of dolomite which continues from the underground powerhouse site. The dolomite contacts with black hard slate at the cliff about 100 m NNW of the outlet of tailrace. The black slate changes to slaty pyhillite and phyllite as it departs from the contact. As the outlet site is near the contact between dolomite and slate, dolomite may intercalate the thin layer of slate and phyllitic slate.

Thick talus deposit is not distributed around the outlet of tailrace.

(3) Geotechnical Evaluation

- 1) The tunnel section from the intake to the middle of the headrace tunnel, which is 70% of the 1,000 m long headrace tunnel, will be composed of phyllite and slaty phyllite. The remaining 30 % of the tunnel will be composed of dolomite. Although the boundary between phyllite and dolomite is presumed to be a fault in the reservoir area, which runs straightly in E-W direction, any phenomenon, which suggest a large fault geologically or topographically, are not observed on the right bank.

The strike of phyllite is almost parallel to the axis of the tunnel and dipping is 45-50 degree. If a seam or fractured zone along the bedding plane of phyllite is predominant, it

is not favorable condition for the tunnel excavation, but it does not bring on the significant difficulties of the tunnel excavation.

- 2) Penstock and underground powerhouse site are composed of dolomite. The thickness of dolomite layer near the underground powerhouse site is estimated to be about 200 m, and the width of the dolomite layer in the horizontal plane is about 300 m. The dolomite layer has enough wide distribution for the layout of the underground powerhouse and penstock. As the observation results of the outcrops, dolomite in this area is hard and relatively a few jointed, and it is evaluated as a good rock condition. However, the rock condition and the distribution of dolomite in deep portion are not directly confirmed. In May 2007, NEA is carrying out the investigation drillings in the vicinity of the underground powerhouse site. Accordingly, it is necessary to examine the investigation drilling results carried out by NEA and to confirm the rock condition and the distribution of dolomite by the exploratory adit and the investigation drillings in the adit during the detailed design stage.
- 3) As the outlet of tailrace is composed of dolomite same as the underground powerhouse, there seems to be no large problem for the construction works.

7.3.5 Estimated Mechanical Properties of the Foundation Rock

(1) Laboratory Test Results of the Drilled Cores

Laboratory test results of the drilled cores are shown in **Table 7.3.5-1**, **Table 7.3.5-2** and **Table 7.3.5-3**. Specific gravity, absorption, uniaxial compression strength and tensile strength of dolomite and slate/phyllite are as follows;

Dolomite

Specific gravity; 2.64 to 2.82 (2.74 in average), Absorption; 0.17 to 0.79 (0.38 in average)

Uniaxial compression strength; 20 to 100 MPa (54 MPa in average)

Tensile strength; 6.9 to 20 MPa (14.8 MPa in average)

Slate/Phyllite

Specific gravity; 2.67 to 2.78 (2.71 in average), Absorption; 0.27 to 0.69 (0.52 in average)

Uniaxial compression strength; 16 to 105 MPa (59 MPa in average)

Tensile strength; 7.6 to 18.7 MPa (14.2 MPa in average)

Large variation of uniaxial compression strength of dolomite and slate/phyllite is considered to be caused by the micro cracks and shistosity in the test specimens.

Table 7.3.5-1 Physical Properties of the Drilled Core

Drill Hole No.	Depth (m)	Rock Type	Specific Gravity	Absorption %
B - 2	25.00 - 25.55	Dolomite	2.75	0.52
B - 2	59.15 - 59.75	Dolomite	2.76	0.43
B - 2	99.00 - 99.50	Dolomite	2.74	0.35
B - 5	37.55 - 38.10	Dolomite	2.75	0.35
B - 5	63.65 - 64.50	Dolomite	2.72	0.19
B - 7	33.00 - 33.50	Dolomite	2.76	0.37
B - 9	32.00 - 32.50	Dolomite	2.75	0.17
B - 9	85.00 - 85.30	Dolomite	2.75	0.36
BP-1	64.00 - 64.40	Dolomite	2.64	0.32
BH-1	44.00-45.00	Dolomite	2.82	0.54
BH-2	36.65-37.55	Dolomite	2.73	0.14
BH-2	47.35-48.00	Dolomite	2.71	0.45
BH-3	49.55-50.00	Dolomite	2.73	0.79
Average			2.74	0.38
BH-2	4.00-5.00	Dolomite (Fragment in Colluvium)	2.66	0.38
BH-3	3.50-4.00	Dolomite (Fragment in Colluvium)	2.75	0.84
BH-5	5.50-6.00	Dolomite (Fragment in Colluvium)	2.66	1.44
Average			2.69	0.89
BH-1	24.65-25.00	Dolomitic Quarzite	2.62	0.38
BH-5	26.00-26.50	Dolomitic Quartzite (Fragment in Colluvium)	2.74	0.48
BH-6	5.10-5.70	Quartzite (Fragment in Colluvium)	2.71	0.24
Average			2.69	0.37
BH-4	43.53-44.00	Slate/Phyllitic Slate	2.68	0.27
BH-5	42.00-43.00	Phyllitic Schist	2.67	0.61
BH-6	22.13-22.50	Phyllite	2.78	0.69
Average			2.71	0.52

Table 7.3.5-2 Tensile Strength of the Drilled Core

Hole No	Hole Depth (m)	Rock Type	Tensile Strength (MPa)
BH-1	7.28 to 7.50	Dolomite	6.9
BH-1	8.65 to 8.93	Dolomite	8.6
BH-1	14.41 to 14.64	Dolomite	13.9
BH-1	30.15 to 30.51	Dolomite	20.0
BH-1	30.63 to 30.89	Dolomite	15.9
BH-1	31.03 to 31.30	Dolomite	19.6
BH-6	31.60 to 31.84	Dolomite	13.8
BH-6	32.17 to 32.46	Dolomite	15.9
BH-6	32.50 to 32.76	Dollomite	18.9
Average			14.8
BH-1	25.08 to 25.39	Dolomitic Quarzite	20.7
BH-1	27.67 to 27.98	Dolomitic Quarzite	20.2
BH-1	29.30 to 29.60	Dolomitic Quarzite	19.3
Average			20.1
BH-4	53.80 to 54.10	Slate/Phyllitic Slate	16.2
BH-6	23.48 to 23.82	Phyllite	18.7
BH-6	35.13 to 35.48	Phyllite	7.6
Average			14.2

Table 7.3.5-3 Uniaxial Compressive Strength of the Drilled Core

Name of Drilled Hole	Depth of Sample(m)	Rock Type	Uniaxial Compressive Strength (MPa)	Remarks
B-2	25.0 - 25.5	Dolomite	72.3	
B-2	59.15 - 59.75	Dolomite	91.6	
B-2	99.0 - 99.5	Dolomite	77.8	
B-3	11.35 - 11.70	Dolomite	42.8	
B-3	55.68 - 56.17	Dolomite	44.8	
B-3	97.70 - 98.10	Dolomite	35.1	
B-4	18.55 - 19.00	Dolomite	89.9	
B-4	54.17 - 54.50	Dolomite	140.2	*-1) Crystallized
B-4	104.78 - 105.16	Dolomite	60.0	
B-5	37.55 - 38.10	Dolomite	49.5	
B-5	63.65 - 64.5	Dolomite	22.3	
B-7	33.0 - 33.5	Dolomite	14.8	*-2) Foliation
B-9	32.0 - 32.5	Dolomite	74.5	
B-9	85.0 - 85.5	Dolomite	34.8	
BP-1	64.00 - 64.40	Dolomite	19.9	
BH-1	4.24 to 4.39	Dolomite	99.0	
BH-1	17.00 to 17.15	Dolomite	78.0	
BH-1	37.35 to 37.51	Dolomite	24.6	
Average			53.9	
BH-1	8.33 to 8.50	Dolomitic Quartzite	125.7	
BH-1	15.47 to 15.61	Dolomitic Quartzite	13.7	
BH-1	24.17 to 24.35	Dolomitic Quartzite	169.4	
BH-6	8.35 to 8.56	Schistose quartzite	22.9	
Average			82.9	
BH-4	44.76 to 44.89	Slate/Phyllitic Slate	82.8	
BH-4	48.86 to 49.00	Slate/Phyllitic Slate	75.5	
BH-4	51.65 to 51.79	Slate/Phyllitic Slate	104.7	
BH-4	83.22 to 83.37	Slate/Phyllitic Slate	17.3	
BH-6	26.00 to 26.17	Pyllite	3.1	*-2) Foliation
BH-6	36.47 to 36.59	Pyllite	15.5	
Average			59.1	

*-1): High compressive strength because of the crystallization. This data is excluded from the average.

*-2): Low compressive strength because of remarkable foliation. This data is excluded from the average.

(2) Estimated Mechanical Properties of the Foundation Rocks

As the in-situ rock mechanical test is not carried out in the project area, the mechanical properties of the foundation rocks are estimated from the rock evaluation described in 7.3.2(2) and RMR (Rock Mass rating).

As for the dam site and the underground powerhouse, the rock evaluation and RMR are obtained from the results of the geological reconnaissance, investigation drillings and the laboratory test of the drilled core. And the mechanical properties of the foundation rocks are estimated from the relation between the rock evaluation and the mechanical properties of the rock mass indicated in **Table 7.3.5-4**, the relation of the RMR and the modulus of the elasticity (Hoek and Brown 1997), and the relation between RMR and the shear strength of the rock mass (Bieniawski 1979, Aydan 2000). On the other hand, no geological

investigation works are carried out for the waterway and underground powerhouse of Option III b except for the intake site. Accordingly, the rock evaluation and RMR of the Option III b are decided based on the result of the geological reconnaissance. The mechanical properties of the waterway and underground powerhouse of Option III b are estimated in a manner same to the dam site. Estimated mechanical properties of the foundation rocks are shown in **Table 7.3.5-5**.

Table 7.3.5-4 Rock Mass Classification and Mechanical Properties

Rock Class	Modulus of deformation	Modulus of elasticity	Shear strength	
	(kgf/cm ²)	(kgf/cm ²)	τ_0 (kgf/cm ²)	ϕ (Degree)
A – B	> 50,000	> 80,000	> 40	55 - 65
CH	50,000 – 20,000	80,000 – 40,000	40 - 20	40 - 55
CM	20,000 – 5,000	40,000 – 15,000	20 - 10	30 - 45
CL	< 5,000	< 15,000	< 10	15 - 38

(Kikuchi et al, 1984, JSEG ; Rock Mass Classification, Engineering Geology Special Issue.)

Table 7.3.5-5 Estimated Mechanical Properties of Foundation Rocks

	Dam			Option II				Option IIIb			
				Underground Powerhouse				Underground Powerhouse	Wtaerway		
	River bed	Left bank	Right bank	Arch		Lower portion of Cavern			Dolomite	Rock Cover is less than 40m	Rock Cover is larger than 40m
Strength of intact rock	50-100 Mpa	50-100 Mpa	50-100 Mpa	50-100 Mpa	50-100 Mpa	25-50 Mpa	25-50 Mpa	50-100 Mpa	50-100 MPa	25-50 Mpa	50-100 MPa
Rating	7	7	7	7	7	4	4	7	7	4	7
RQD	<25%, 25-50%	25-50%, 50-	<25%	< 25%	< 25%	< 25%	< 25%	25-50%	25-50%	< 25%	< 25%
Rating	5.5	10.5	3	3	3	3	3	8	8	3	3
Spacing of discontinuities	6-20cm, 20-60cm	20 - 60cm	6 - 20cm	6 – 20 cm	6 – 20 cm	< 6cm	< 6cm	6-20cm, 20-60cm	6-20cm, 20-60cm	< 6cm	6 – 20 cm
Rating	9	10	8	8	8	5	5	9	9	5	8
Condition of discontinuities	S.R & S.W.	S.R & S.W.	S.R & S.W to S.R.& H.W.	S.R & S.W.	S.R & S.W.	S.R & H.W.	S.R & H.W to Slickesided	S.R & S.W.	S.R & S.W.	S.R & H.W.	S.R & S.W.
Rating	25	25	22.5	25	25	20	15	25	25	20	25
Groundwater condition	—	—	—	Damp	Damp	Damp	Damp	Damp	Damp	Damp	Damp
Rating	—	—	—	10	10	10	10	10	10	10	10
Discontinuity orientation	—	—	—	Fair	Unfavourable	Fair	Unfavourable	Fair	Fair	Unfavourable	Unfavourable
Rating	—	—	—	-5	-10	-5	-10	-5	-5	-10	-10
RMR	54.7	61.8	47.6	48	43	37	27	54	54	32	43
	Good to Fair	Good	Fair	Fair	Fair	Poor	Poor	Fair	Fair	Poor	Fair
Rock Evaluation	CH	CH-B	CH-CM	CM	CM	CL	CL	CH	CH	CM-CL	CM-CH
Rock Type	Dolomite	Dolomite	Dolomite	Dolomite	Dolomite	Dolomite	Dolomite	Dolomite	Dolomite	Slate/Phyllite	Slate/Phyllite
σ_c (MPa)	35 - 100 (Ave. 65)										
Specific Gravity	2.64 - 2.82 (Ave. 2.74)										
Absorption (%)	0.17 - 0.79 (Ave. 0.38)										

Estimated Modulus of elasticity

Ed (MPa) 1)	7,900	11,900	5,300	5,400	4,000	2,900	1,600	7,600	7,600	2,100	3,900
Ed (MPa) 2)	4,000-8,000	6,000-8,000<	2,700-6,000	1,500-4,000	1,500-4,000	<1,500	<1,500	4,000-8,000	4,000-8,000	<1,500 - 2,700	2,700-6,000

Estimated Shear strength

C (MPa) 3)	2 - 3	3 - 4	2 - 3	2 - 3	2 - 3	1 - 2	1 - 2	2 - 3	2 - 3	1 - 2	2 - 3
C (MPa) 2)	2 - 4	3 - 4<	1.5 - 3	1 - 2	1 - 2	< 1	< 1	2 - 4	2 - 4	< 1 - 1.5	1.5 - 3
ϕ (Degree) 3-*)	25 - 35	35 - 45	25 - 35	25 - 35	25 - 35	15 - 25	15 - 25	25 - 35	25 - 35	15 - 25	25 - 35
ϕ (Degree) 2)	40 - 55	48 - 60	38 - 48	30 - 45	30 - 45	15 - 38	15 - 38	40 - 55	40 - 55	26 - 38	38 - 48
ϕ (Degree) 4)	47	51	44	44	42	39	34	47	47	36	42

1) $E_d = (\sqrt{qc}) / 10 \times 10^{(RMR-15)/40}$ Gpa, $qcB < 100MPa$, Hoek and Brown, 1997

2) See **Table 7.3.5-4**

3) Bieniawski, 1979 * Relationship between the shear strength and RMR proposed by Bieniawski is applicable to slopes only in saturated and weathered rock.

The cohesion is one order of magnitude higher in the case of tunnel. (B. Singh & Goel, 1999). According to this statement, C proposed by Bieniawski is decupled in this table. 3-*) Furthermore, Mehrotra, 1993, pointed out that values of Bieniawski are somewhat conservative. According to Mehrotra, 1993, ϕ values are lager than that of Bieniawski. The difference between both ϕ values is more than 10 degree.

4) $\phi = 20 + 0.5 \times RMR$, Aydan, 2000

5) Average uniaxial compressive strength for the calculation Ed 1) excludes the test results affected by micro cracks or shistosity.

7.4 Construction Material

(1) Investigation Works

The investigations of the concrete aggregate had been carried out for the river deposits of the Seti River and the Madi River by NEA. These investigation results are summarized in “Feasibility Study Report on Upper Seti Storage Hydroelectric Project, 2001, by NEA” and “Additional Geological and Geotechnical Investigation Final report, 2005, by NEA”. Investigated area and the investigation volume are shown in **Table 7.4-1**, and the location of the investigation is shown in **Fig.7.4-1**.

Table 7.4-1 Investigation Area for Concrete Aggregate

Name of Area	Location	Number of Test Pits	Number of Sample	Remarks
GMA	Madi River	4	5	Feasibility Study by NEA in 2001
GMB	Madi River	2	2	
GSA	Seti River	4	5	
GSB	Seti River	3	3	
GSC	Seti River	2	3	
GSD	Seti River	2	2	
GSE	Seti River	2	2	
GSAA	Seti River	4	9	Upgrading Feasibility Study by NEA in 2005
GSAB	Seti River	5	16	
GMAA	Madi River	7	10	

(2) Result of the Investigation Works

The results of the investigations are shown in **Table7.4-2** and **Table7.4-3**. As for the grain size distribution, the fine constituents are a little bit large in quantity and the grain size distribution undergoes a change remarkably. The specific gravity is 2.67~2.74, the absorption is 0.15~0.35, the soundness is 0.5~2.1 and the abrasion loss is 29.8~37.3. These results satisfy the standards of ASTM and JIS for the concrete aggregate. The result of Alkali-aggregate reactivity test, chemical method, shows $S_c=530\sim1,300$ mmol/L and $R_c=15\sim65$ mmol/L. This test result indicates that the river deposit and dolomite at the dam site are deleterious aggregate in the Alkali reactivity.

As the result of the investigation, the total volume of the aggregate of 10 investigated areas is about $14,200,000$ m³. Even if the area is selected considering the contents of fine material, the necessary volume of the concrete aggregate for the project, $1,300,000$ m³, is estimated to be secured.

Dolomite distributed in the left bank upstream of the dam site is investigated for the concrete aggregate. The quality of the material is almost same to the river deposit of the Seti River and the Madi River as shown in **Table7.4-2**. As this dolomite layer continues to the dam site, the foundation rock of the dam is estimated to be a same quality of this dolomite.

Table 7.4.2 Test Results of the Concrete Aggregate (2001)

	GMA	GMB	GSA	GSB	GSC	GSD	GSE
Particle Size Distribution							
Gravel (4.76mm <)	0 - 61.5	29.1 - 58.7	6.3 - 70	65.9 - 74.8	0.2 - 35.8	55.5 - 59.6	60.0 - 61.8
Sand	37.4 - 94.4	40 - 68.6	26.1 - 86.8	17.7 - 32.0	62.3 - 93.6	35.8 - 42.7	338.3 - 36.8
Fines (< 0.074mm)	1.0 - 5.6	0.4 - 2.3	4.0 - 8.7	1.3 - 15.2	1.8 - 6.2	1.8 - 4.9	1.4 - 1.7
USCS Classification	GP, SP, SP-SM	GP,SP	GP,SP,GP-GM	GM,GW	SP,SP-SM	GP	GP,GW
Area (m ²)	160,000	700,000	21,000	120,000	74,375	393,125	297,500
Thickness (m)	2.05	2.35	1.75	2.85	2	2.5	2.5
Volume (m ³)	328,000	1,645,000	36,750	342,000	148,750	9,828,125	743,750

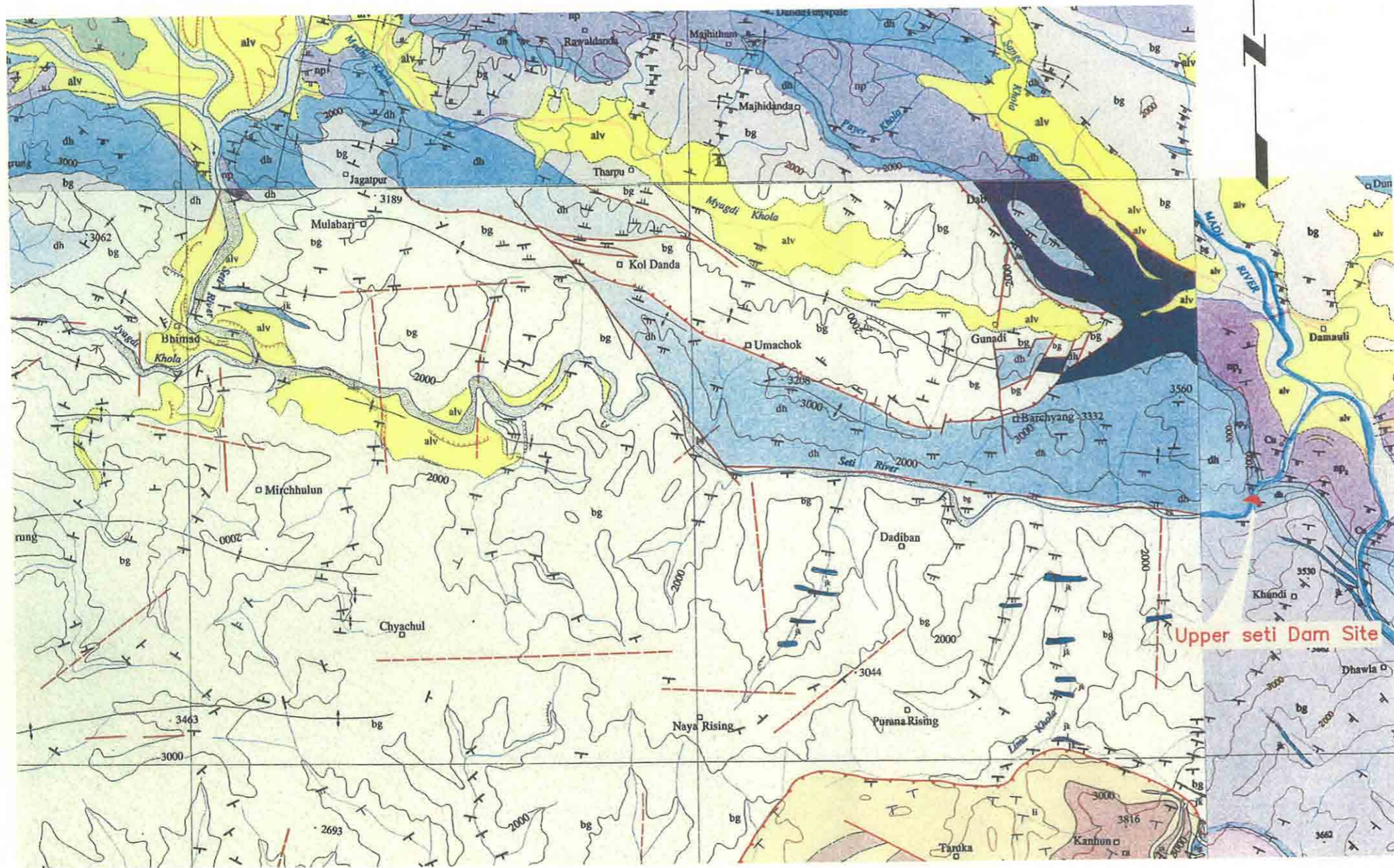
Table 7.4-3 Test Results of the Concrete Aggregate (2005)

	GSA A	GSA B	GMA A	Left bank upstream of dam (Dolomite)
Particle Size Distribution				
Gravel (4.76mm <)	2.5 - 60.2	0.5 - 63.8	1.6 - 63.9	
Sand	5.8 - 47.4	30.1 - 72.8	39.8 - 94.4	
Fines (< 0.074mm)	4.5 - 91.5	2.9 - 65.1	0.1 - 12.1	
USCS Classification	ML,SM,GP,GW	SM,ML,GP,GW	GP,SP,SM,SW	
Soundness(Na2SO4)	1.8 - 2.1	0.5 - 2.5	1.3 - 1.9	1.2 - 1.4
Abration	29.8 - 34.3	28.9 - 33.7	33.9 - 37.3	22.5 - 23.3
Alkali Aggregate Reaction				
Sc mmol/l	527	1305		664 - 693
Rc mmol/l	65	15		32 - 33.3
Dry density	2.73	2.72	2.67 - 2.74	2.67 - 2.70
Absorption	0.15 - 0.30	0.17 - 0.35	0.2 - 0.3	0.15 - 0.23
Area (m ²)	38,500	80,600	427,500	
Thickness (m)	2	3	1.97	
Volume (m ³)	77,000	241,800	842,175	

(3) Geotechnical Evaluation

- 1) The river deposit of the Seti River and the Madi River contains a fine material in some degree. However, it is considered that these materials can be used for the concrete aggregate in selecting the area of few fine materials and washing out the fine components while producing the concrete aggregate. And the necessary volume of the concrete aggregate for the project, 1,300,000 m³, is estimated to be secured. The result of Alkali-aggregate reactivity test indicates the deleterious aggregate for the river deposit and dolomite near the dam site. However, the chemical method of Alkali-aggregate reactivity test is not suitable for the carbonate rock such as dolomite in many cases. Therefore, the detailed investigations including the Mortar-bar method should be carried out and the possibility of the Alkali-aggregate reactivity of the dolomite should be examined during the detailed design stage.

- 2) The excavated rock of the dam foundation may be utilized for the concrete aggregate instead of the river deposit. The investigation results up to now shows that dolomite of the dam foundation is almost same quality to the river deposit, so it is assumed that the dam foundation rock can used for the concrete aggregate. As for the Alkali-aggregate reactivity, the detailed investigation is necessary in the same manner as the river deposit.



LEGEND

SURFICIAL DEPOSITS (Quaternary to Recent)

alv Alluvial Deposits : Silt, sand, gravel in terraces, flood plain and stream - channels.

SIWALIK GROUP (Neogene)

si₃ Upper Siwalik : Conglomerates with subordinate sandstones and shales.

si₂ Middle Siwalik : Sandstone with shale and siltstone.

si₁ Lower Siwalik : Vari-coloured shale with sandstone and siltstone.

U. NAWAKOT GROUP (? U. Paleozoic)

bg Benighat Slates : Dark slates and phyllites, carbonaceous slates with Jhiku carbonates and rare quartzites.

L. NAWAKOT GROUP (U. Precambrian to L. Paleozoic)

dh Dhading Dolomite : Light blue-grey stromatolitic dolomite

Nourpul Formation

np₁ Upper : Pink to light cream dolomitic quartzite to silicious dolomite, thin vari-coloured calc- phyllite and impure quartzite.

np₂ Middle : Grey to dark green and purple phyllites with subordinate impure quartzites, rare white quartzites and minor discontinuous carbonates. Local boulder bed in Phundi Khola.

np₃ Lower : White to greenish grey ripplemarked orthoquartzite to impure quartzite with vari-coloured phyllite intercalations.

dz Dandagaon Phyllite : Green-grey phyllites with rare quartzites and minor carbonates

fg Fagfog Quartzite : White ripplemarked quartzite with minor phyllite intercalations

kn Kunchha Formation : Light green-grey gritty phyllites, quartzitic phyllites, metasandstones and gritstones with minor amphibolites

BHIMPHEDI GROUP (Precambrian)

ra Raduwa Formation : Grey to dark-green, garnetiferous mica-schist with white micaceous quartzite beds.

BASIC ROCK

gd Amphibolite



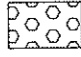
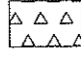
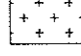
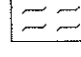
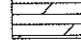
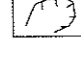
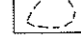
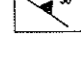
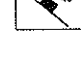
<note> This geological map is compiled from "Geological Map of Parts of TANAHAM and NAWALPARASI Districts" (1/50,000) and "Geological Map of Parts of TANAHAM, GORKHA and NAWALPARASI Districts" (1/50,000) published by Department of mines and Geology, Nepal, 1999 & 1996.

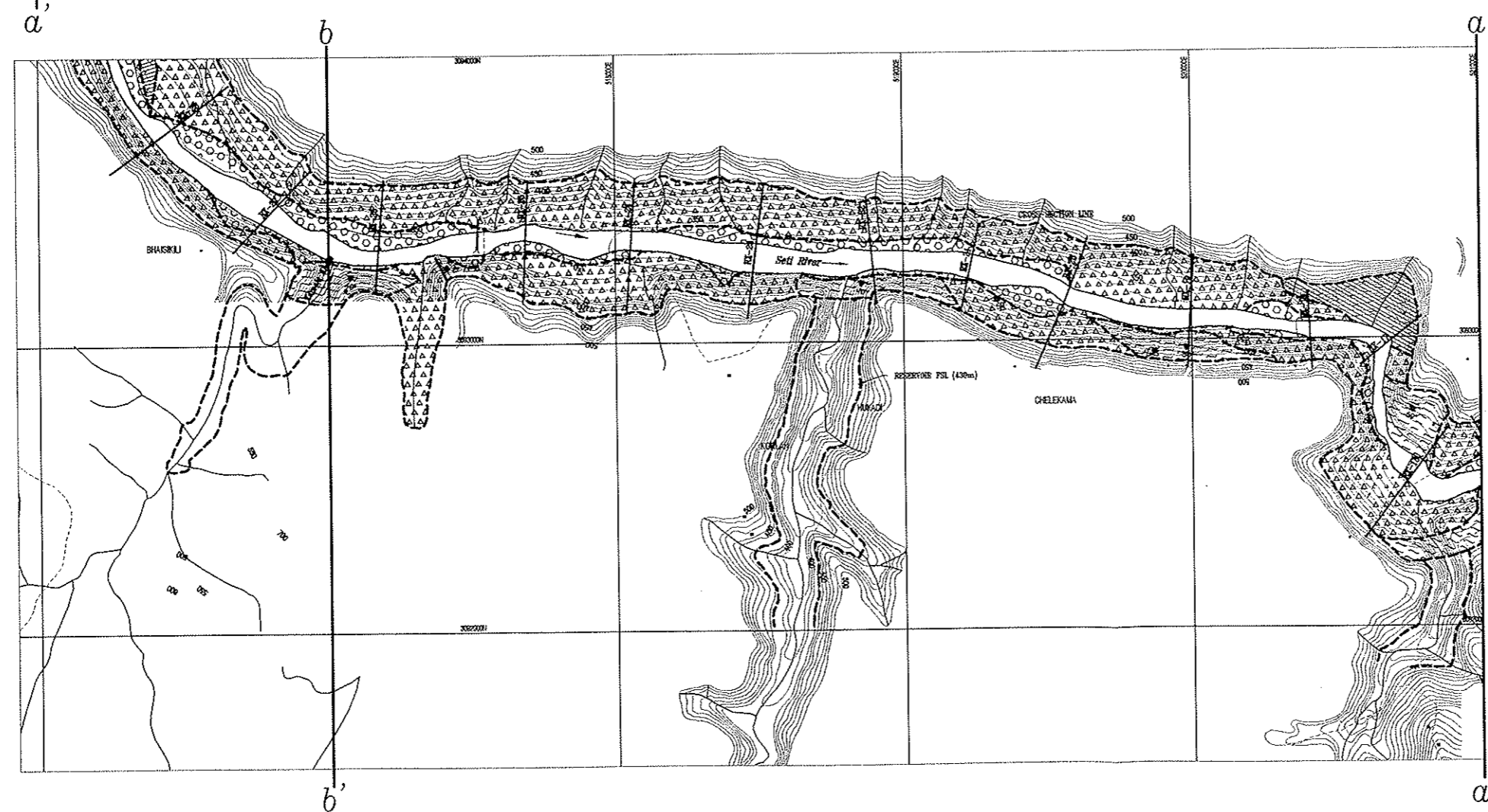
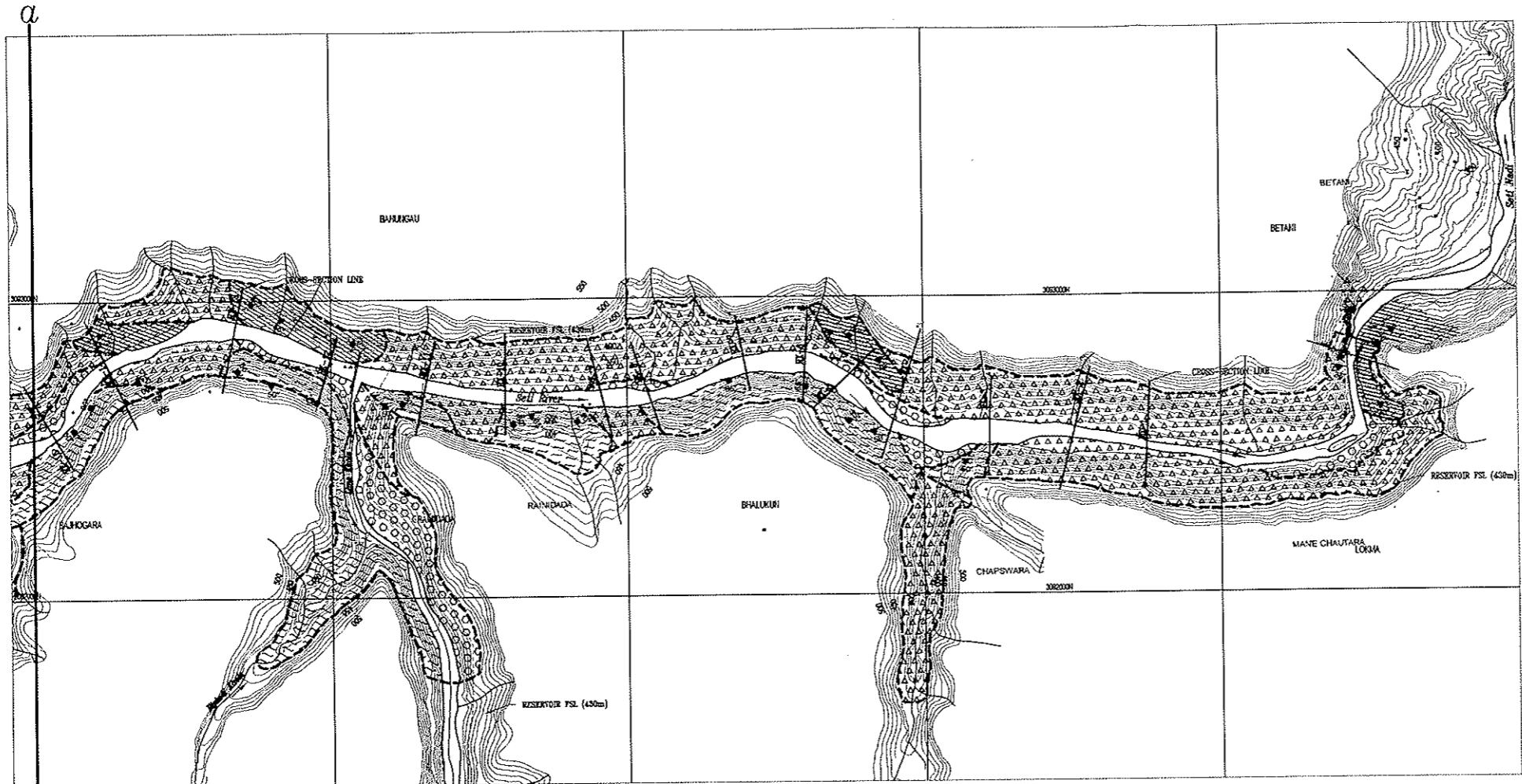
Upgrading Feasibility Study on
Upper Seti (Damauli)
Hydroelectric Project, NEPAL

**GEOLOGIC PLAN
OF
PROJECT AREA**

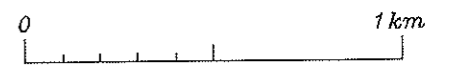
Fig. : 7.1-1 | Date : June, 2007

L E G E N D

-  ALLUVIUM
-  COLLUVIUM
-  RESIDUAL SOIL
-  PHYLLITE
-  DOLOMITE
-  LAND SLIDE
-  GEOLOGICAL BOUNDARY
-  ATTITUDE OF FOLIATION
-  ATTITUDE OF JOINTS


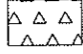
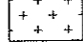
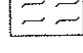
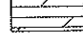
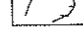
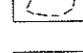
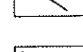
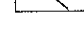


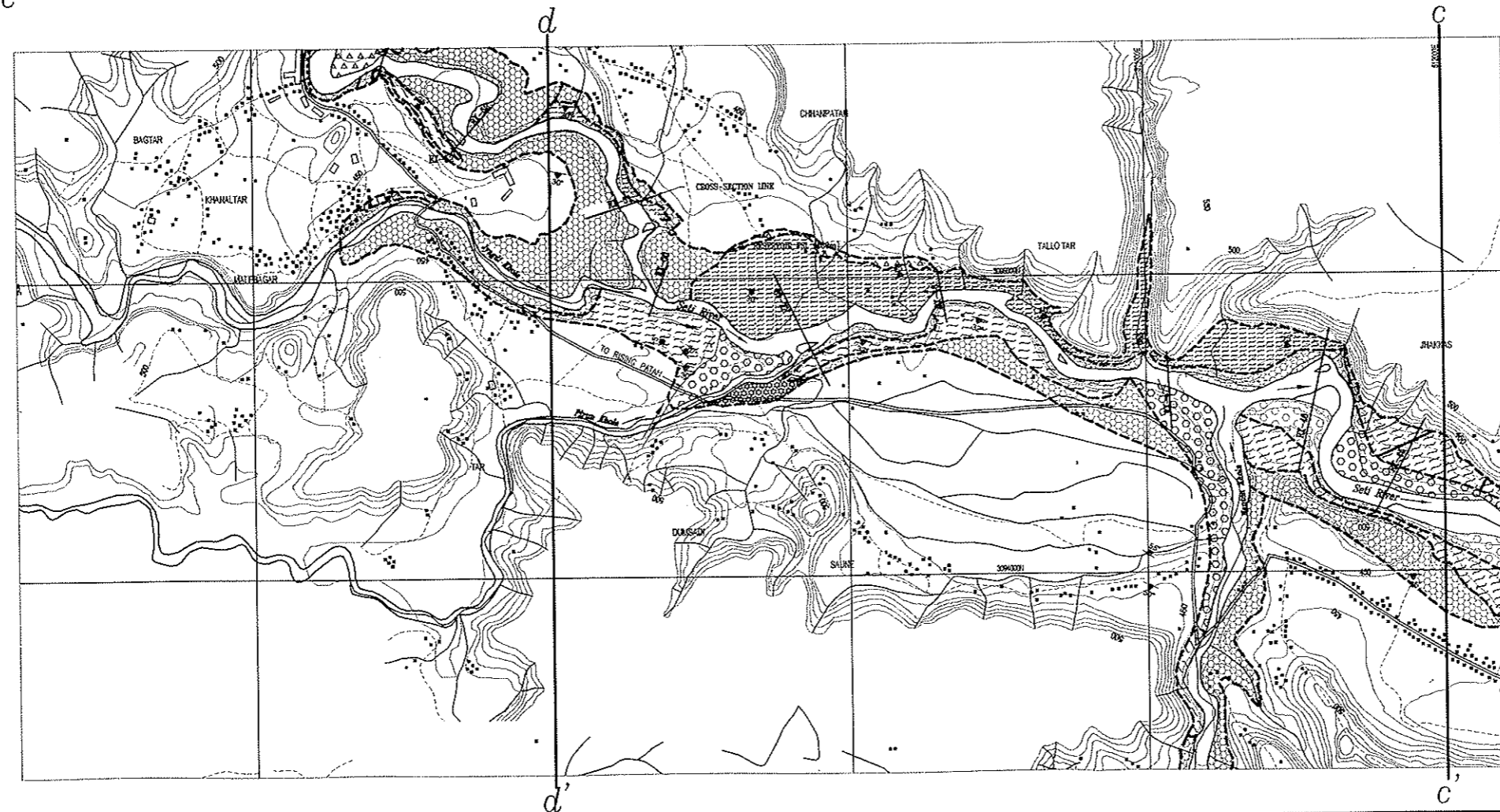
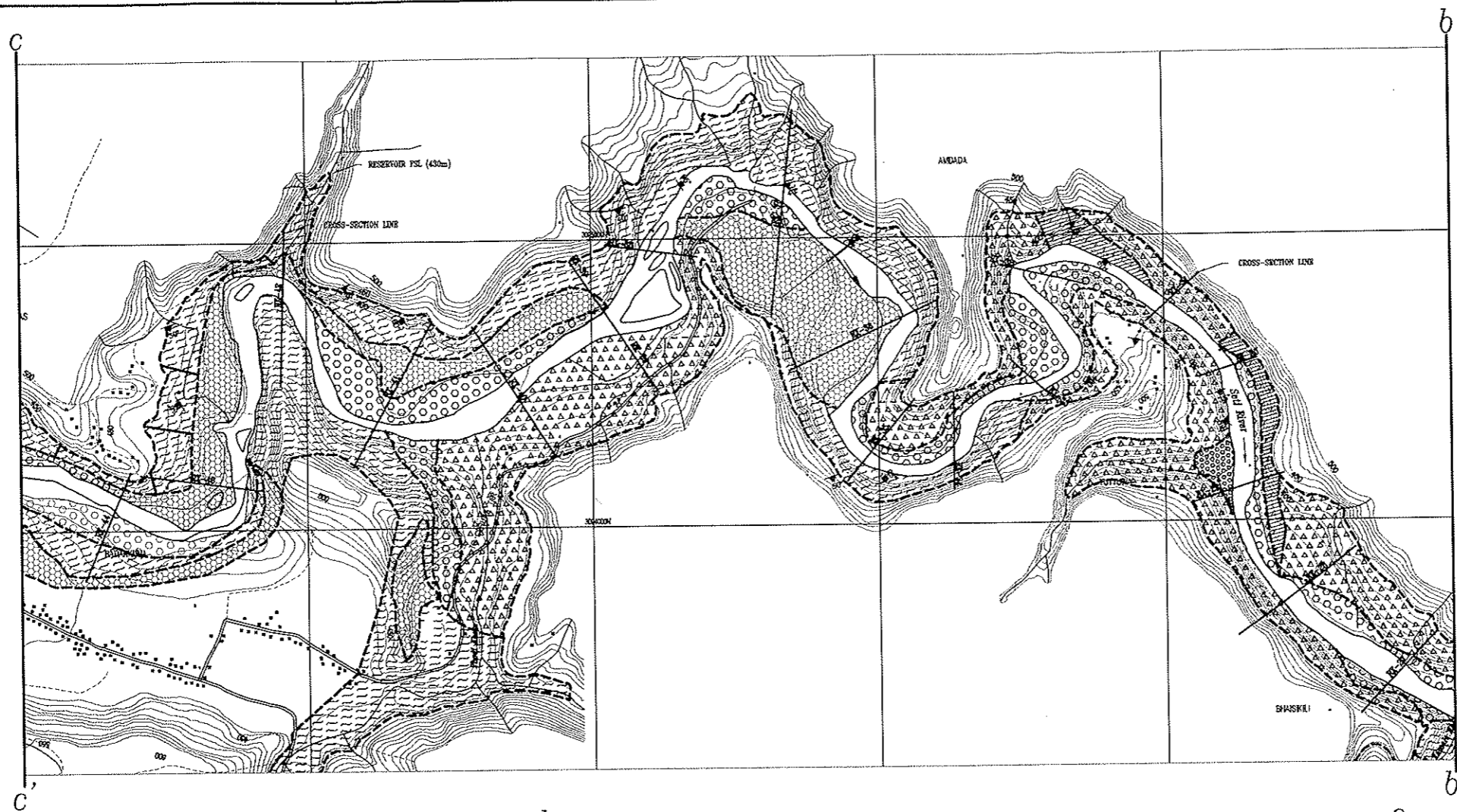
<SOURCE>
 Additional Geological and Geotechnical Investigation
 Final Report, 2005 by NEA



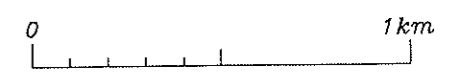
Upgrading Feasibility Study on Upper Seti (Damauli) Hydroelectric Project, NEPAL	
GEOLOGIC MAP OF RESERVOIR AREA(1/3)	
Fig. : 7.3.1-1	Date : June, 2007

L E G E N D

-  ALLUVIUM
-  COLLUVIUM
-  RESIDUAL SOIL
-  PHYLLITE
-  DOLOMITE
-  LAND SLIDE
-  GEOKOCICAL BOUNDARY
-  ATTITUDE OF FOLIATION 30°
-  ATTITUDE OF JOINTS 40°



<SOURCE>
 Additional Geological and Geotechnical Investigation
 Final Report , 2005 by NEA


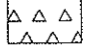
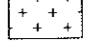
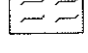
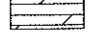
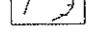
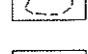
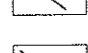
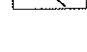


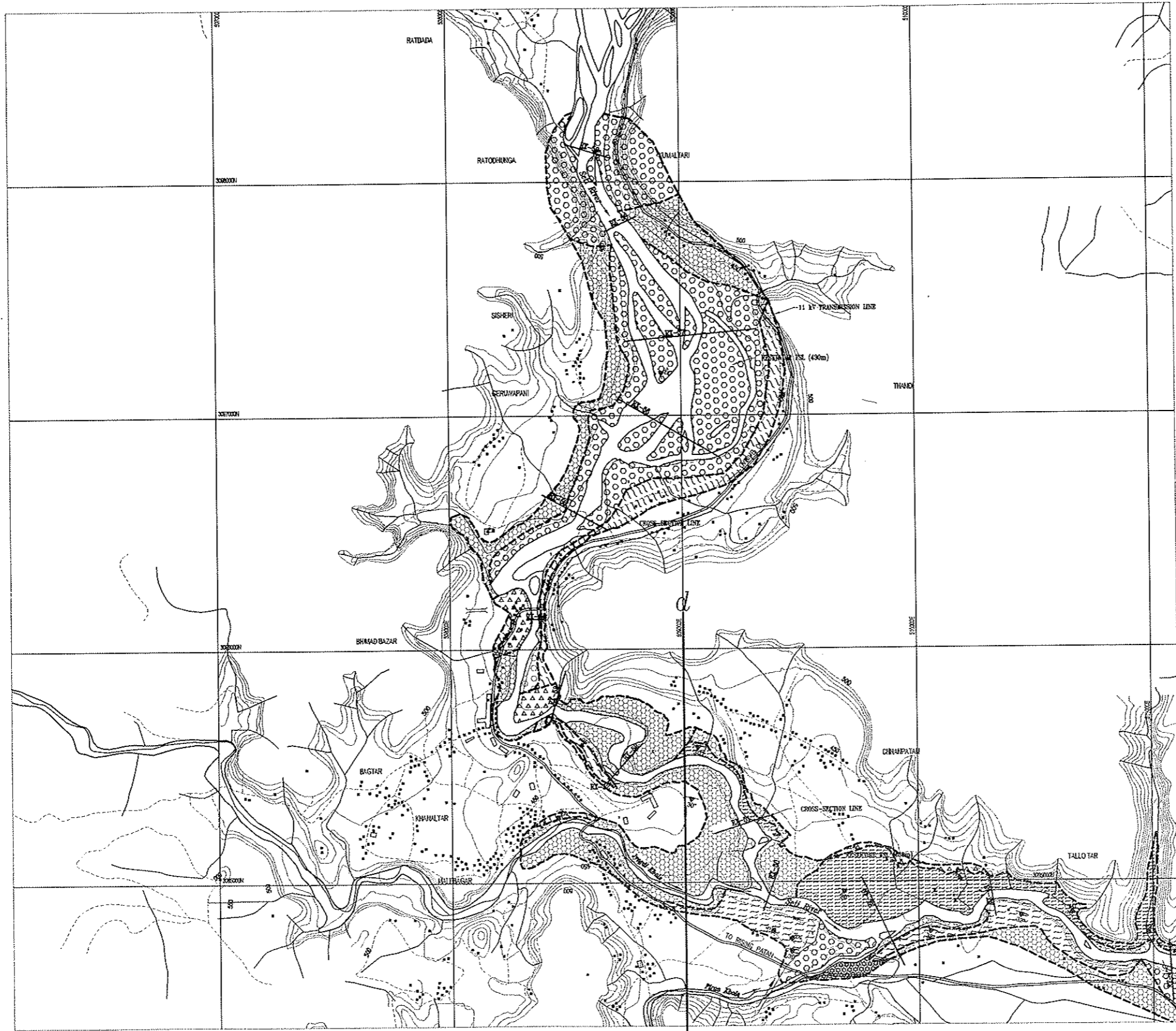
Upgrading Feasibility Study on
 Upper Seti (Damauli)
 Hydroelectric Project , NEPAL

**GEOLOGIC MAP
 OF
 RESERVOIR AREA(2/3)**

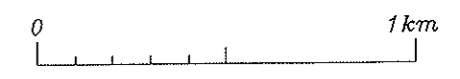
Fig. : 7.3.1-2 | Date : June,2007

L E G E N D

-  ALLUVIUM
-  COLLUVIUM
-  RESIDUAL SOIL
-  PHYLLITE
-  DOLOMITE
-  LAND SLIDE
-  GEOLOGICAL BOUNDARY
-  ATTITUDE OF FOLIATION 30°
-  ATTITUDE OF JOINTS 40°



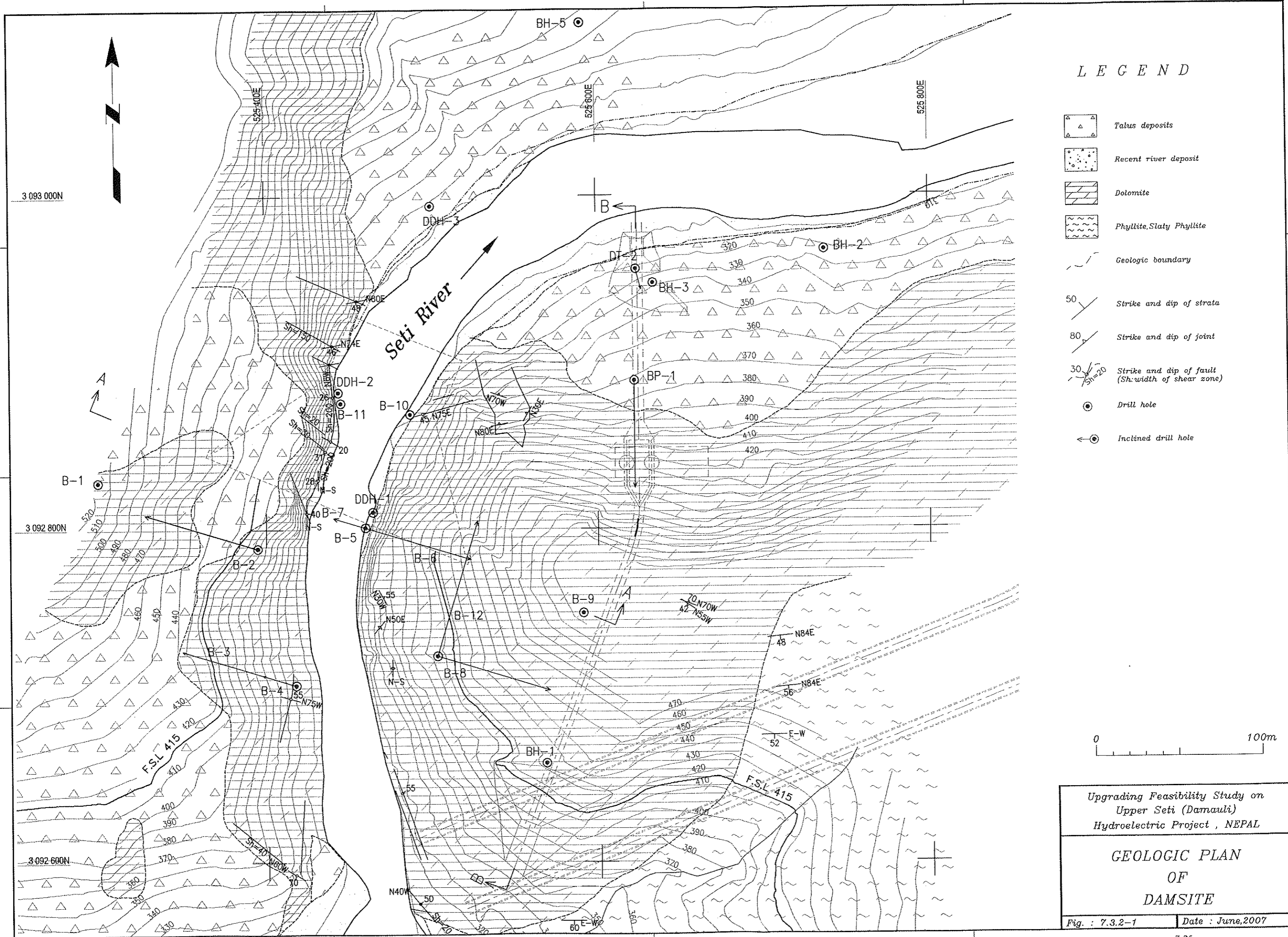
<SOURCE>
 Additional Geological and Geotechnical Investigation
 Final Report, 2005 by NEA



Upgrading Feasibility Study on
 Upper Seti (Damauli)
 Hydroelectric Project, NEPAL

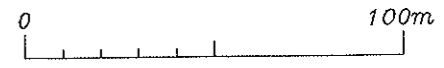
GEOLOGIC MAP
 OF
 RESERVOIR AREA(3/3)

Fig. : 7.3.1-3 Date : June, 2007



LEGEND

- Talus deposits
- Recent river deposit
- Dolomite
- Phyllite, Slaty Phyllite
- Geologic boundary
- 50° Strike and dip of strata
- 80° Strike and dip of joint
- 30° Strike and dip of fault (Sh. width of shear zone)
- Drill hole
- Inclined drill hole



Upgrading Feasibility Study on
Upper Seti (Damauli)
Hydroelectric Project, NEPAL

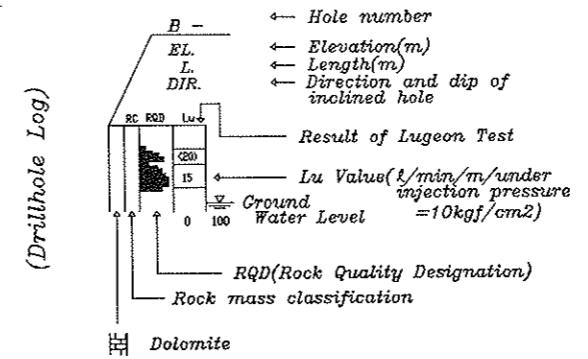
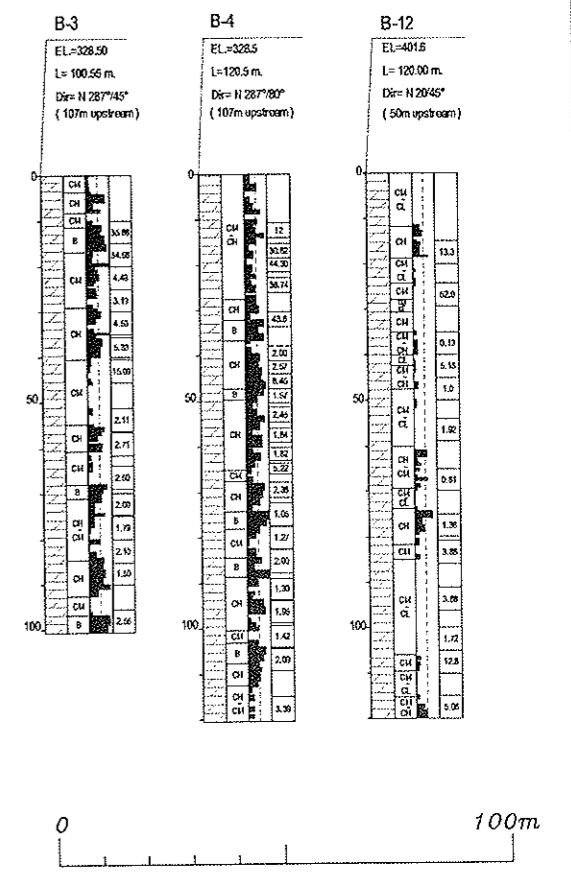
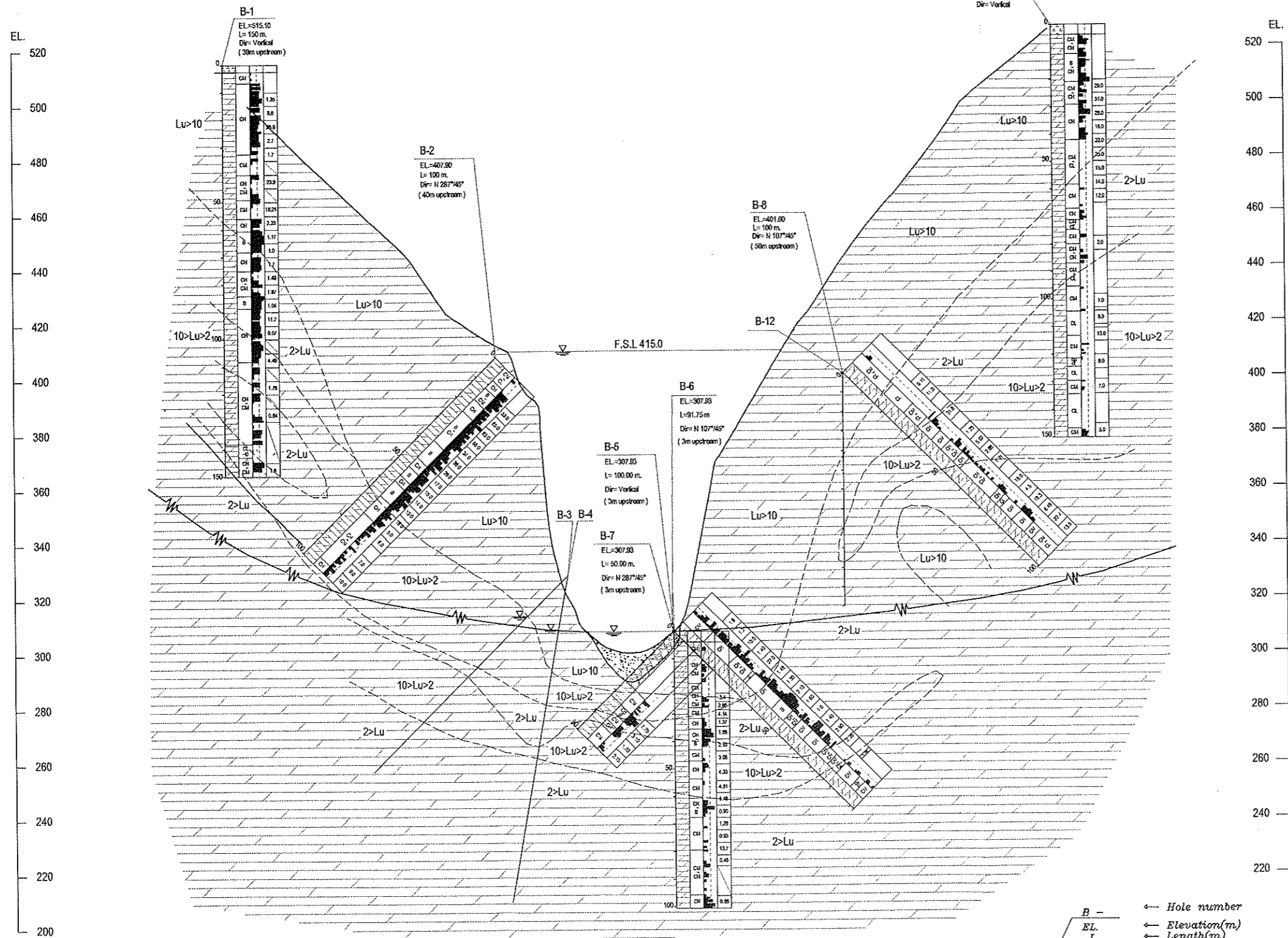
GEOLOGIC PLAN
OF
DAMSITE

Fig. : 7.3.2-1 | Date : June, 2007

A-A

LEGEND

- Talus deposits
- Recent river deposit
- Dolomite
- Ground water level
- Lugeon Value and its boundary




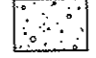
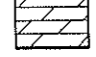
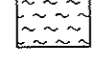
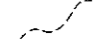
Upgrading Feasibility Study on
Upper Seti (Damauli)
Hydroelectric Project, NEPAL

GEOLOGIC SECTION OF DAMSITE (A - A)




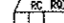

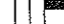


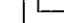
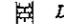

Fig. : 7.3.2-2 Date : June, 2007

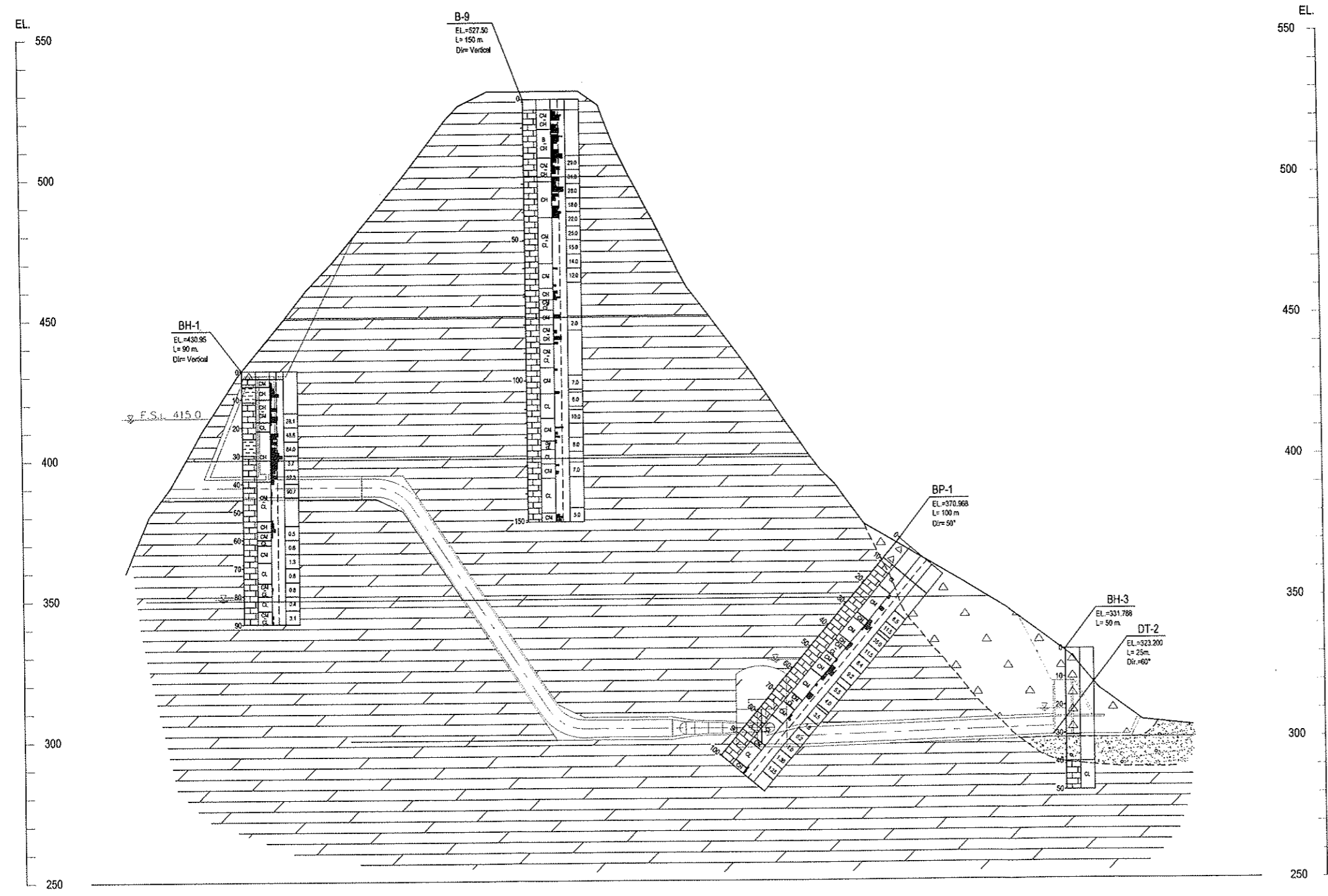
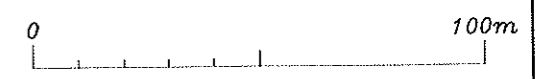
B-B

LEGEND

-  Talus deposits
-  Recent river deposit
-  Dolomite
-  Phyllite, Slaty Phyllite
-  Geologic boundary

(Drillhole Log)

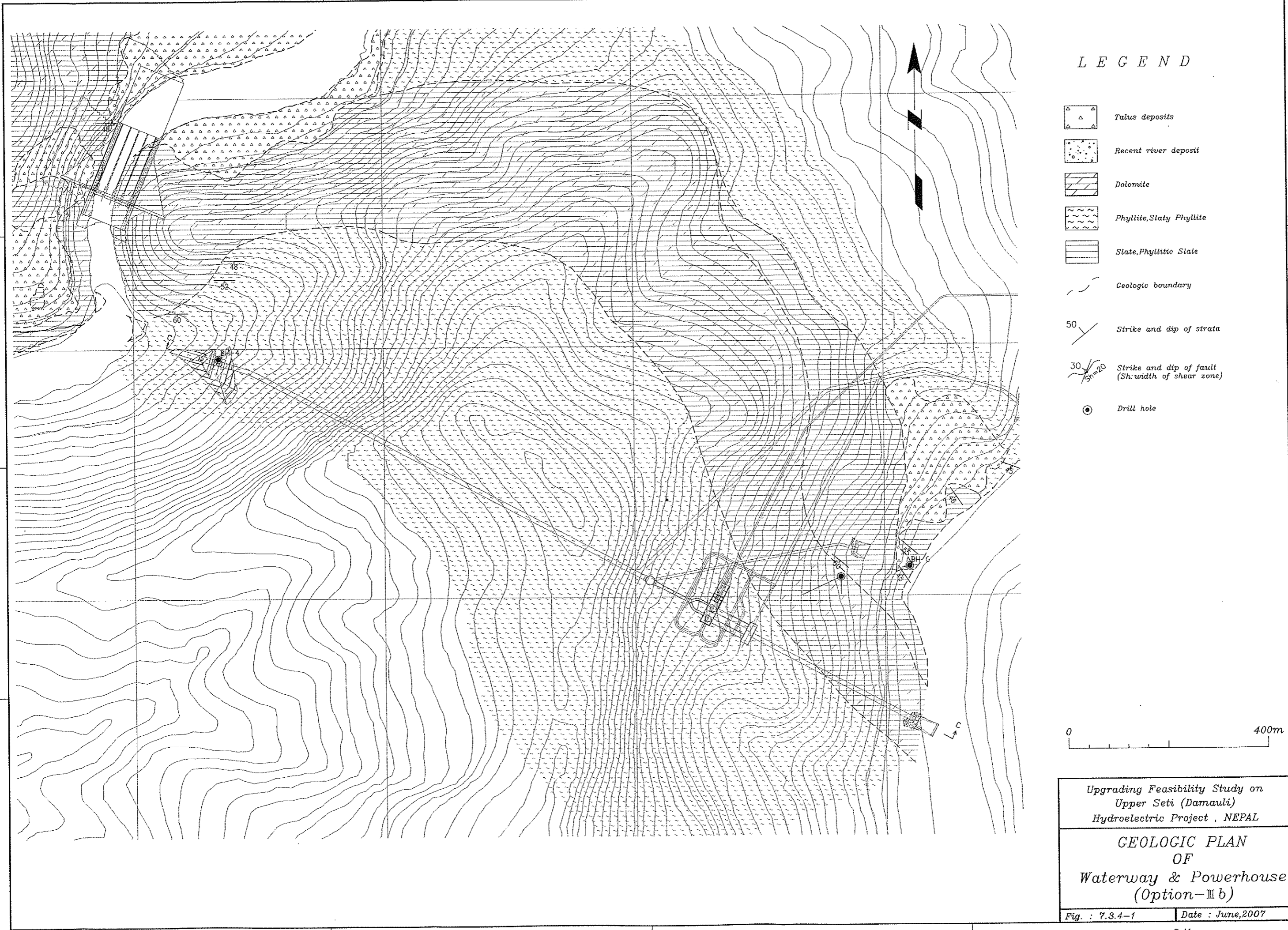
-  Hole number
-  Elevation(m)
-  Length(m)
-  Direction and dip of inclined hole
-  Result of Lugeon Test
-  Lu Value(l/min/m/under injection pressure = 10kgf/cm²)
-  Ground Water Level
-  RQD(Rock Quality Designation)
-  Rock mass classification
-  Dolomite
-  Quartzite, Dolomitic Quartzite.



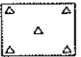

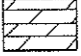
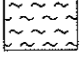
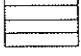
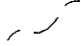
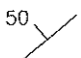
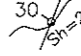

Upgrading Feasibility Study on
Upper Seti (Damauli)
Hydroelectric Project, NEPAL

**GEOLOGIC PROFILE
OF
Waterway & Powerhouse
(Option-II)**

Fig. : 7.3.3-1 Date : June, 2007



L E G E N D

-  Talus deposits
-  Recent river deposit
-  Dolomite
-  Phyllite, Slaty Phyllite
-  Slate, Phyllitic Slate
-  Geologic boundary
-  50 / Strike and dip of strata
-  30 / Sh=20 / Strike and dip of fault (Sh: width of shear zone)
-  Drill hole

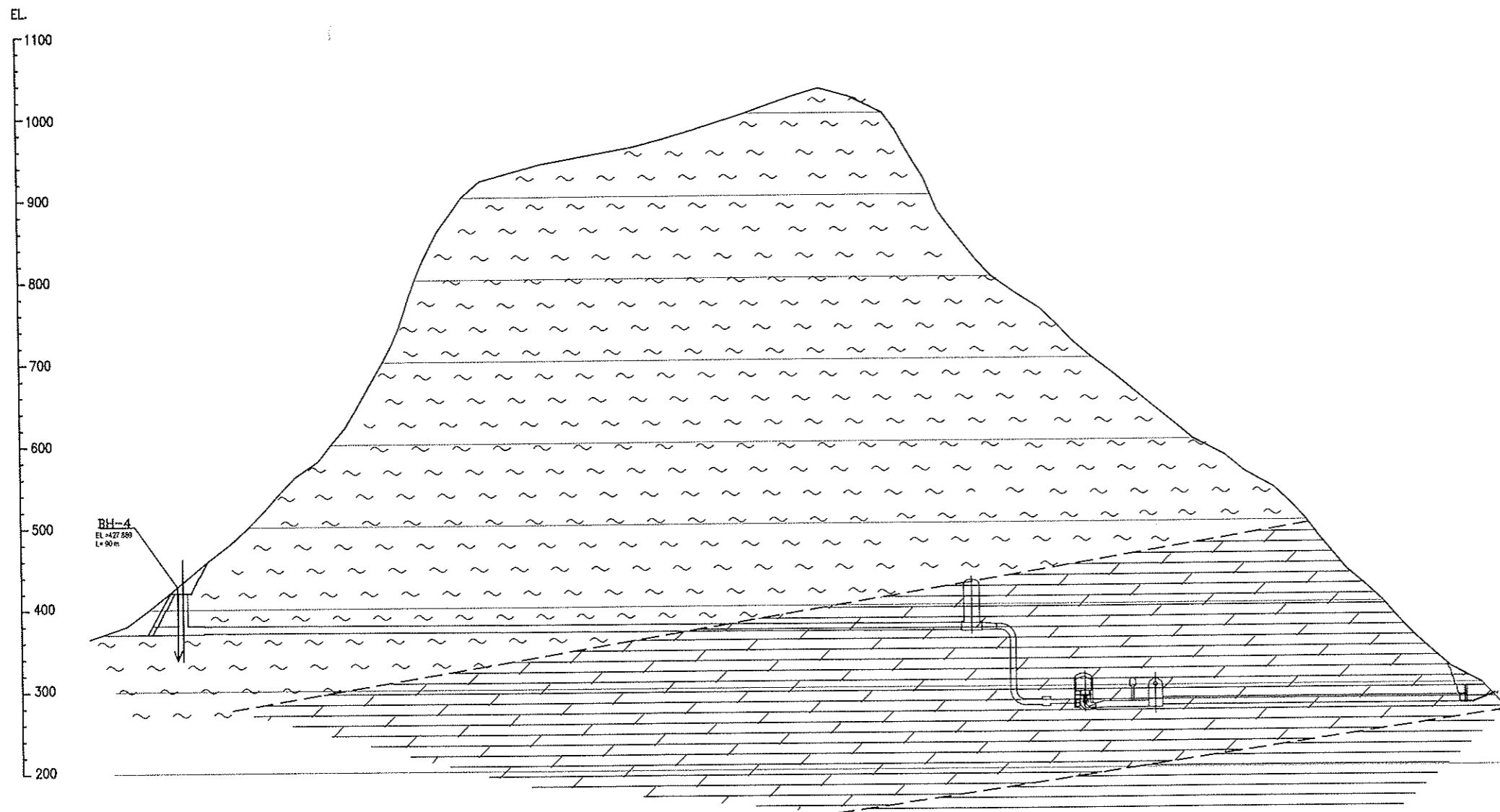
0 400m

Upgrading Feasibility Study on
Upper Seti (Damauli)
Hydroelectric Project, NEPAL

GEOLOGIC PLAN
OF
Waterway & Powerhouse
(Option-III b)

Fig. : 7.3.4-1 Date : June, 2007

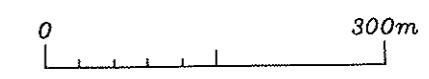
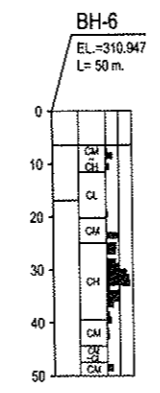
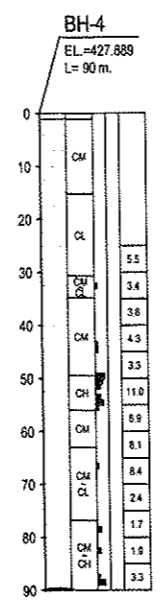
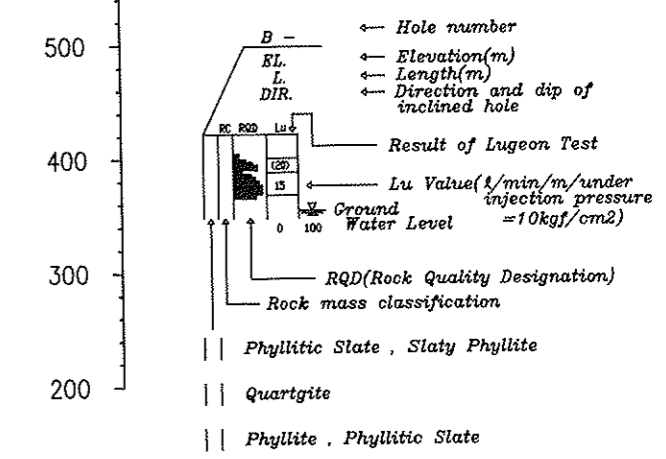
C-C



LEGEND

- EL. 1100
 - 1000
 - 900
 - 800
 - 700
 - 600
 - 500
 - 400
 - 300
 - 200
- Talus deposits
 - Recent river deposit
 - Dolomite
 - Phyllite, Slaty Phyllite
 - Slate, Phyllitic Slate
 - Geologic boundary

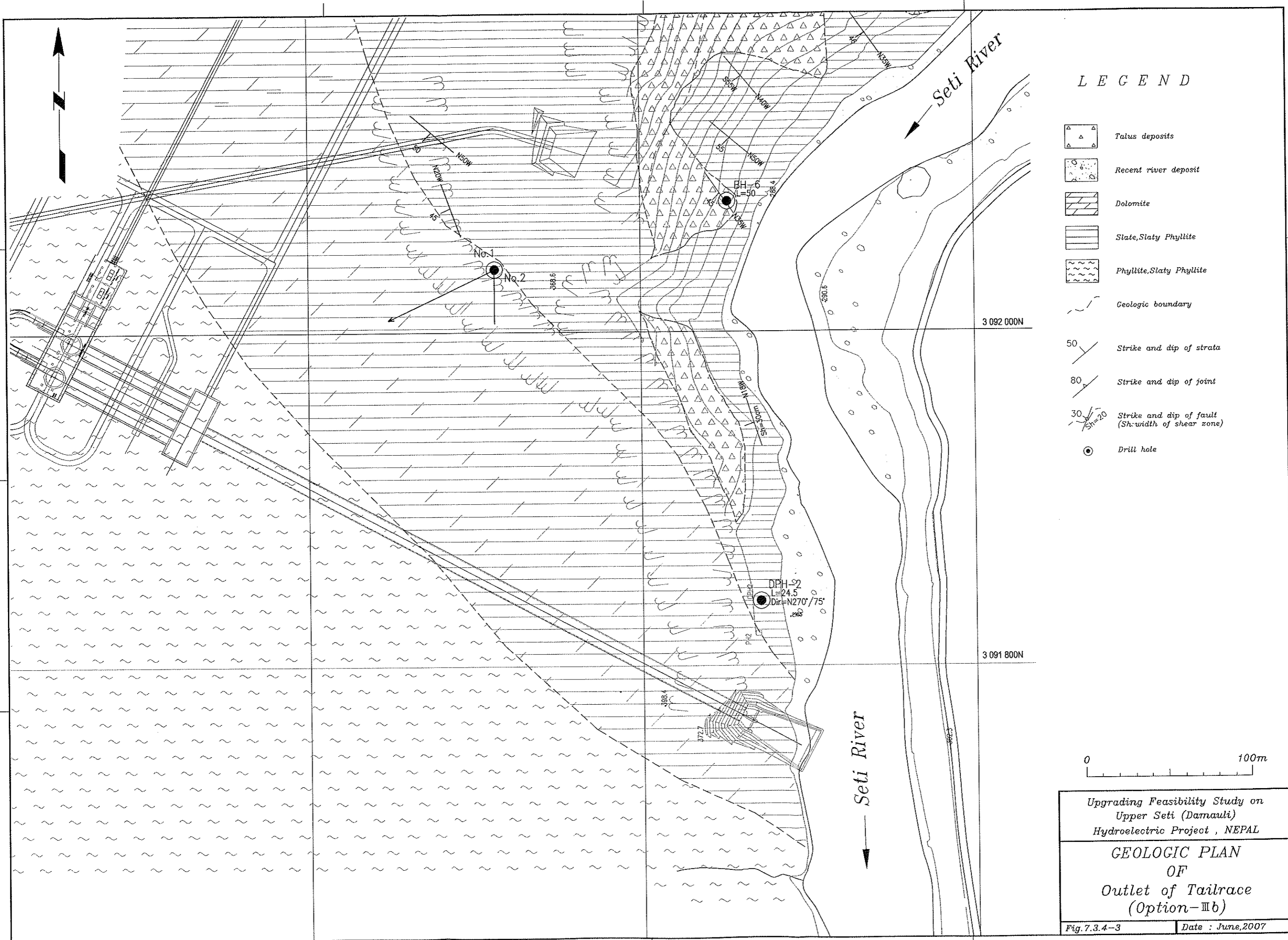
(Drillhole Log)



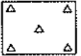

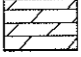
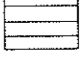
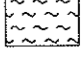

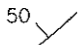
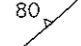
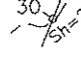

Upgrading Feasibility Study on
Upper Seti (Damauli)
Hydroelectric Project, NEPAL

**GEOLOGIC PROFILE
OF
Waterway & Powerhouse
(Option-IIIb)**

Fig. : 7.3.4-2 Date : June, 2007



L E G E N D

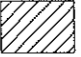

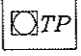
-  Talus deposits
-  Recent river deposit
-  Dolomite
-  Slate, Slaty Phyllite
-  Phyllite, Slaty Phyllite
-  Geologic boundary
-  50 Strike and dip of strata
-  80 Strike and dip of joint
-  30/20 Strike and dip of fault (Sh:width of shear zone)
-  Drill hole

Upgrading Feasibility Study on
Upper Seti (Damauli)
Hydroelectric Project, NEPAL

GEOLOGIC PLAN
OF
Outlet of Tailrace
(Option-IIIb)

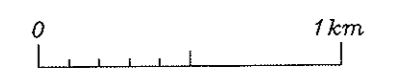
Fig.7.3.4-3 Date: June,2007

L E G E N D

-  Granular Borrow Area ^{※-1}
(GSAA, CSAB and GMAA)
-  Granular Borrow Area ^{※-2}
(GSA ~ GSE)
-  PITS

※-1: Upgrading Feasibility Study Report
by NEA, 2005

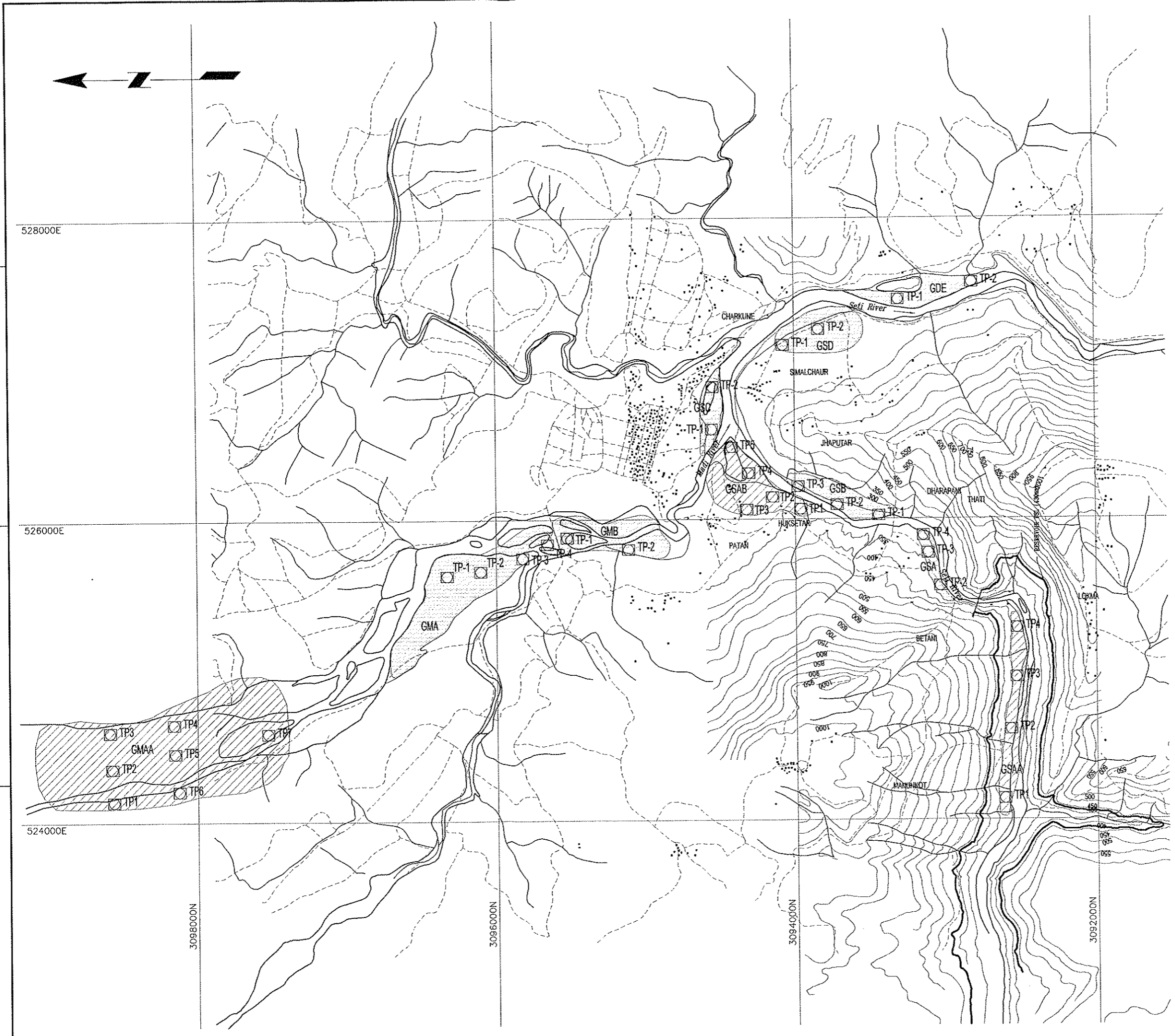
※-2: Feasibility Study Report
by NEA, 2001



Upgrading Feasibility Study on
Upper Seti (Damauli)
Hydroelectric Project, NEPAL

**LOCATION MAP
OF
Investigation for
Concrete Aggregate**

Fig. : 7.4-1 | Date : June, 2007



CHAPTER 8 SEISMOLOGY

CONTENTS

CHAPTER 8	SEISMICITY.....	8-1
8.1	Seismic Activities.....	8-1
8.1.1	Historical Earthquakes in Nepal and the Surrounding Area	8-1
8.2	Seismic Risk Analysis	8-1
8.2.1	Seismic Risk Analysis Based on the Stochastic Approach	8-2
8.2.2	Estimation of Maximum Acceleration at the Dam Site	8-12
8.2.3	Design Horizontal Seismic Coefficient	8-19

LIST OF TABLES

Table 8.1.1-1	Earthquakes in the Himalayan area of Magnitude over 7.5 since 1897.....	8-1
Table 8.2.1-1	Occurrence Frequency of Magnitude among the Collected Data.....	8-2
Table 8.2.1-2	Occurrence Frequency of Seismic Center Depth among the Collected Data.....	8-7
Table 8.2.2-1	Annual Maximum Acceleration during Observation.....	8-13
Table 8.2.2-2	Maximum Acceleration Value by Each Equation to the Advent Period	8-14
Table 8.2.3-1	Basic Seismic Coefficient in the Indian Seismic Hazard Region	8-21
Table 8.2.3-2	Summary of Maximum Acceleration Estimation at the Upper Seti Dam Site	8-21
Table 8.2.3-3	Seismic Coefficient Based Upon Maximum Acceleration	8-22
Table 8.2.3-4	Result of Seismic Coefficient Estimation obtained in Various Ways	8-23

LIST OF FIGURES

Fig. 8.2.1-1	Epicenter Distribution of Earthquakes of Magnitude less than 3	8-4
Fig. 8.2.1-2	Epicenter Distribution of Earthquakes of Magnitude 3 to 4.....	8-4
Fig. 8.2.1-3	Epicenter Distribution of Earthquakes of Magnitude 4 to 5.....	8-5
Fig. 8.2.1-4	Epicenter Distribution of Earthquakes of Magnitude 5 to 6.....	8-5
Fig. 8.2.1-5	Epicenter Distribution of Earthquakes of Magnitude 6 to 7.....	8-6
Fig. 8.2.1-6	Epicenter Distribution of Earthquakes of Magnitude more than 7.....	8-6
Fig. 8.2.1-7	Epicenter Distribution of Earthquakes less than 6 km in Depth.....	8-8
Fig. 8.2.1-8	Epicenter Distribution of Earthquakes between 6 and 10 km in Depth.....	8-8
Fig. 8.2.1-9	Epicenter Distribution of Earthquakes between 10 and 20 km in Depth.....	8-9
Fig. 8.2.1-10	Epicenter Distribution of Earthquakes between 20 and 40 km in Depth.....	8-9
Fig. 8.2.1-11	Epicenter Distribution of Earthquakes between 40 and 60 km in Depth.....	8-10
Fig. 8.2.1-12	Epicenter Distribution of Earthquakes between 60 and 80 km in Depth.....	8-10
Fig. 8.2.1-13	Epicenter Distribution of Earthquakes between 80 and 100 km in Depth.....	8-11
Fig. 8.2.1-14	Epicenter Distribution of Earthquakes more than 100 km in Depth.....	8-11
Fig. 8.2.2-1	Maximum Acceleration for the Return Period by Equation (1).....	8-15
Fig. 8.2.2-2	Maximum Acceleration for the Return Period by Equation (2).....	8-16
Fig. 8.2.2-3	Maximum Acceleration for the Return Period by Equation (3).....	8-17
Fig. 8.2.2-4	Maximum Acceleration for the Return Period by Equation (4).....	8-18
Fig. 8.2.3-1	Seismic Hazard Map in Nepal	8-19
Fig. 8.2.3-2	Seismic Hazard Map in India	8-20
Fig. 8.2.3-3	Seismic Hazard Map in Nepal	8-23

CHAPTER 8 SEISMICITY

8.1 Seismic Activities

8.1.1 Historical Earthquakes in Nepal and the Surrounding Area

Table 8.1.1-1 shows great earthquakes of magnitude more than 7.5 which have occurred since 1897 in Nepal and its surrounding area. Well-known historical earthquakes, which caused severe disasters, were the Assam Earthquake, of magnitude 8.7, on June 12, 1897, the Kangra Earthquake, of magnitude 8.6 on April 4, 1905, the Bihar Earthquake, of magnitude 8.4 on January 12, 1934, the Quetta Earthquake, of magnitude 7.6 on May 30, 1935, and the Assam Earthquake, of magnitude 8.7 on August 15, 1950.

Table 8.1.1-1 Earthquakes in the Himalayan area of Magnitude over 7.5 since 1897

Occurrence date	Latitude (North degrees)	Longitude (Earth degrees)	Location	Magnitude	Seismic center depth (m)
1897.06.12	25.9	91.8	Assam	8.7	1,600
1905.04.04	33.0	76.0	Kangra Valley	8.6	19,000
1908.12.12	26.5	97.0	Burma	7.5	
1916.08.28	30.0	81.0	Far Western Nepal	7.5	
1918.07.08	24.5	91.0	Assam	7.6	
1934.01.15	26.5	86.5	Bihar-Nepal	8.4	11,000
1935.05.30	29.5	66.7	Quetta	7.6	30,000
1947.07.29	28.5	94.0	NE Assam	7.9	
1950.08.15	28.5	96.7	Assam	8.7	1,526

These great earthquakes occurred in the Sindhu – Gung alluvial plain, which comes into contact with the Himalayan tectonic zone along its southern boundary.

Earthquakes are attributable to the continuous catastrophic failure of rocks under strains generated by the relative movements of lithospheric plates. The Himalayan tectonic zone is an area of such plate boundaries, where the Indian and Eurasian plates converge.

8.2 Seismic Risk Analysis

Seismic risk analysis is defined as forecasting the seismic characteristics which will occur at a specific location (site) for a certain period. When forecasting earthquakes or earthquake motion which will occur in future, such forecasts are carried out based on some uncertain factors. For this reason, efforts to decrease this uncertainty are made, based on perspectives involving the clarification of the physical background affecting each phenomena and accumulation of data for the base of quantitative evaluations. It is important to indicate the characteristics of earthquake motion with a “risk index” to show its occurrence possibility.

Stochastic indexes, such as those illustrating the potential for annual occurrence and the return period, are widely used for the risk index. However, this concept does not definitively insist that the occurrence of earthquakes indicates a stochastic phenomenon by nature. It is meaningful to extrapolate the issue to an estimation of risk index by regarding the relative frequency (probability distribution) of uncertain factors, which exist in the quantitative evaluation of related parameters.

Seismic risk analysis based on the stochastic method is generally considered an efficient engineering approach, with a clear meaning and explicit interpretation of its result. This approach is also widely applied to determining the horizontal seismic coefficient for the seismic design of dams, hence it is used in the Study and its procedure is as described in the following sections.

8.2.1 Seismic Risk Analysis Based on the Stochastic Approach

The seismic data used in the Study are based on those from 1994 to 2004 by the National Seismological Center in Nepal and those from 1905 to 1995 by the NOAA (National Oceanic and Atmospheric Administration), United States Department of Commerce. The above data files include details of around 4,000 earthquakes which had their epicenters located within a 1,000 km radius of the Upper Seti Project site (84° 15' 30" in East Longitude and 27° 57' 14" in North Latitude). As mentioned in 8.1.1, earthquake events in Nepal are mainly considered attributable to the geodynamic process of plate collision and crustal shortening in the Himalayas. The seismic data collected for the Study also show that epicenters are distributed in the Himalayan Tectonic zone as described below.

The following show seismic characteristics in the project site and its surrounding area, based on the collected data:

- (1) Epicenter Distribution by Magnitude

Table 8.2.1-1 shows the frequency occurrence of magnitude among the collected data.

Table 8.2.1-1 Occurrence Frequency of Magnitude among the Collected Data

Magnitude	Number of data	Amount
<3	69	69
<4	137	206
<5	2,479	2,685
<6	1,010	3,695
<7	315	4,010
<8	50	4,060
Total	4,060	

Figs. 8.2.1-1 ~ 8.2.1-6 show the epicenter distribution of the earthquakes listed in **Table 8.2.1-1** by magnitude. The following are summarized based on the epicenter distributions:

- Earthquakes with epicenters located in Nepal, of magnitude 4 to 5, are overwhelming.

- Earthquakes with epicenters located in Nepal, of magnitude 5 to 6, following the above
- Almost all epicenters located in Nepal are distributed in the Himalayan tectonic zone.
- No earthquakes exceeding 7 in magnitude occurred near the project site.

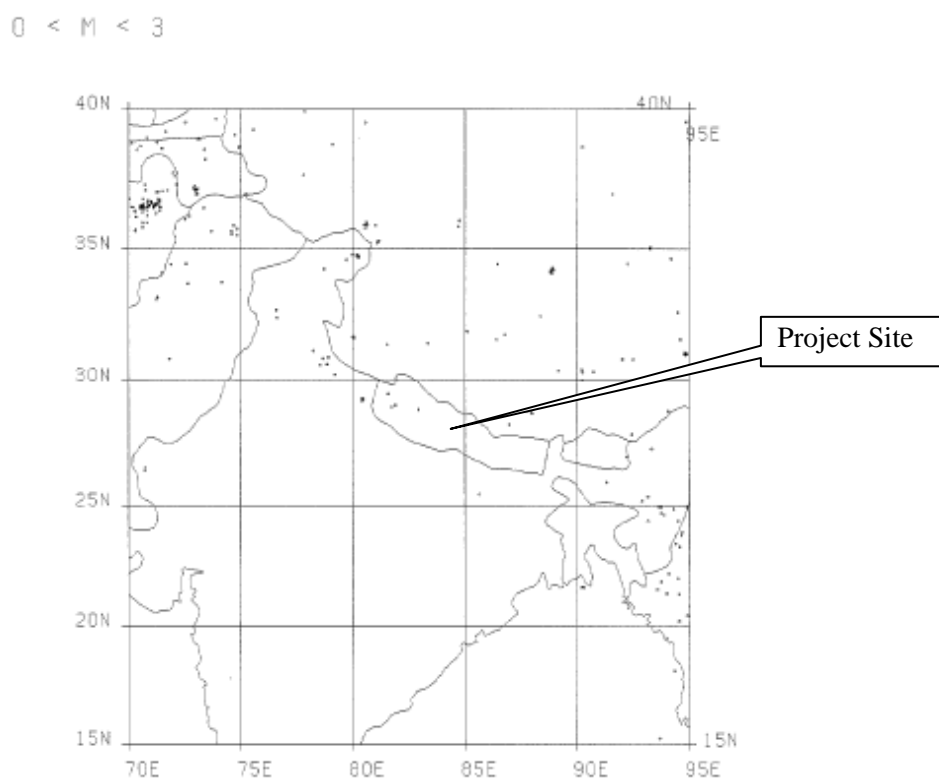


Fig. 8.2.1-1 Epicenter Distribution of Earthquakes of Magnitude less than 3

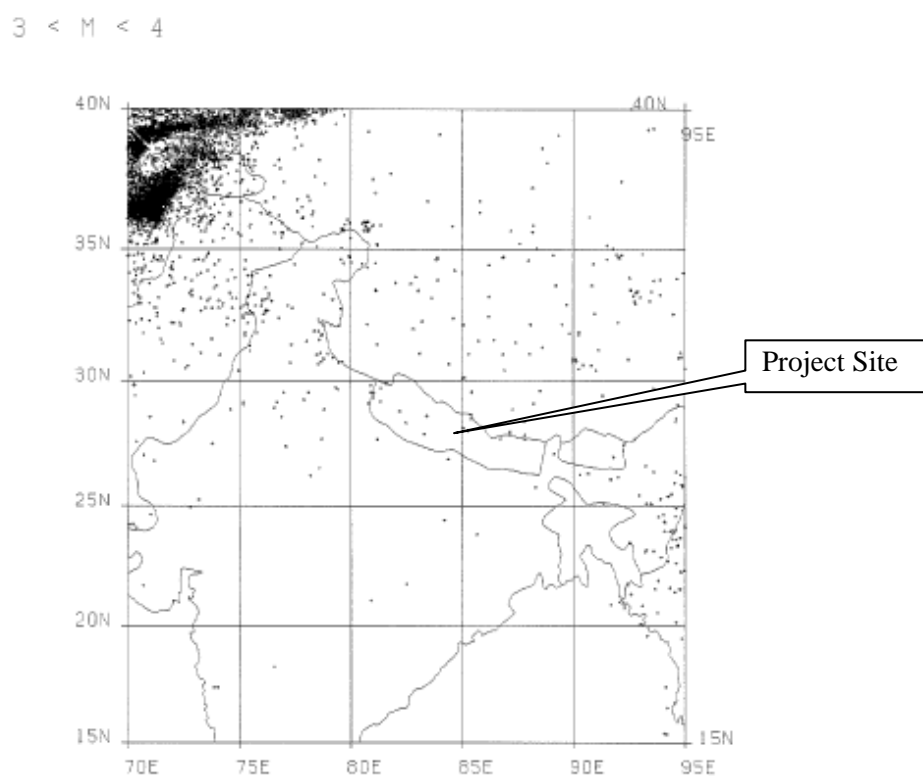


Fig. 8.2.1-2 Epicenter Distribution of Earthquakes of Magnitude 3 to 4

4 < M < 5

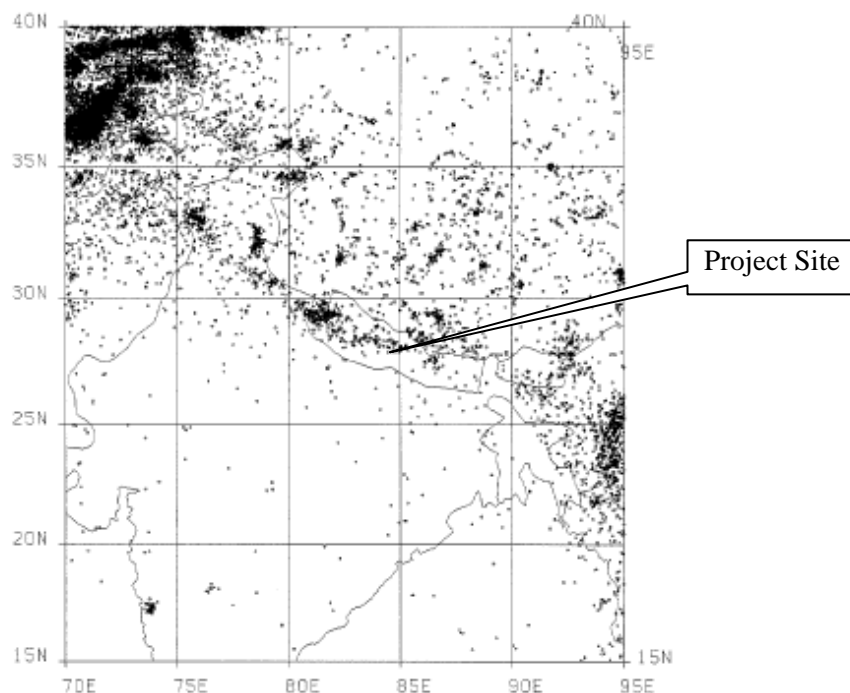


Fig. 8.2.1-3 Epicenter Distribution of Earthquakes of Magnitude 4 to 5

5 < M < 6

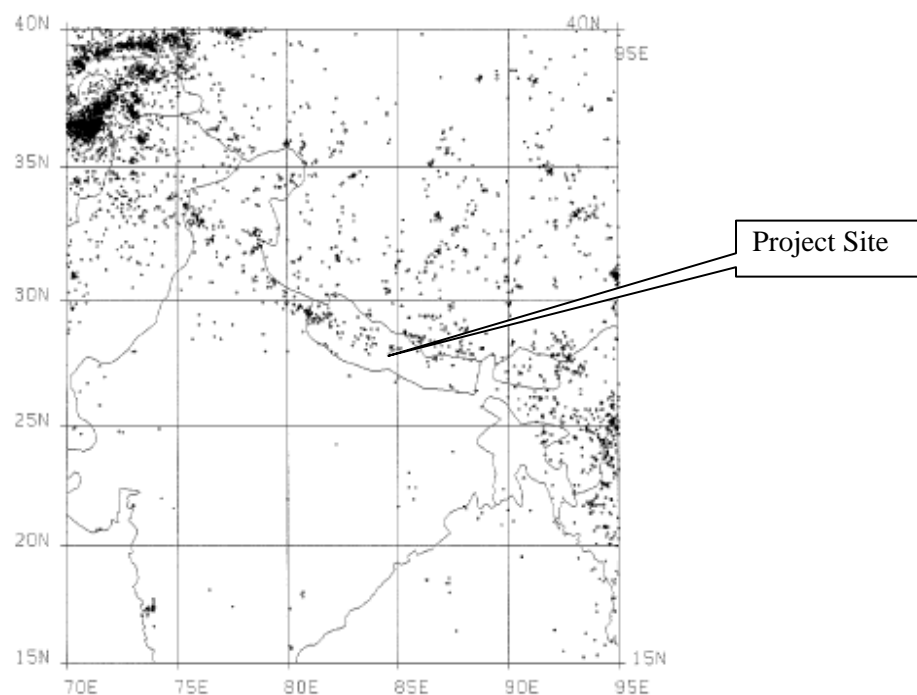


Fig. 8.2.1-4 Epicenter Distribution of Earthquakes of Magnitude 5 to 6

6 < M < 7

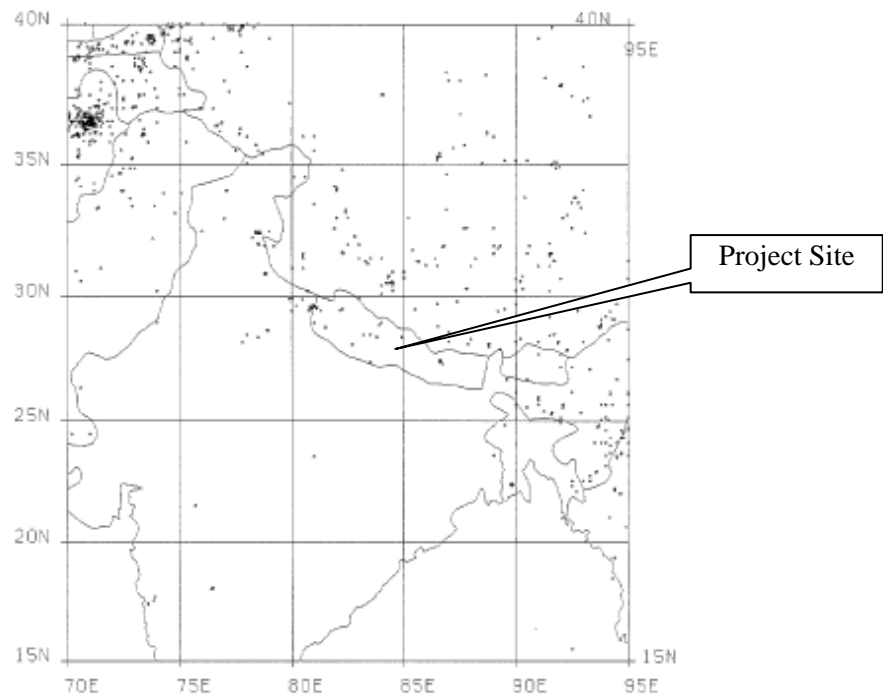


Fig. 8.2.1-5 Epicenter Distribution of Earthquakes of Magnitude 6 to 7

7 < M

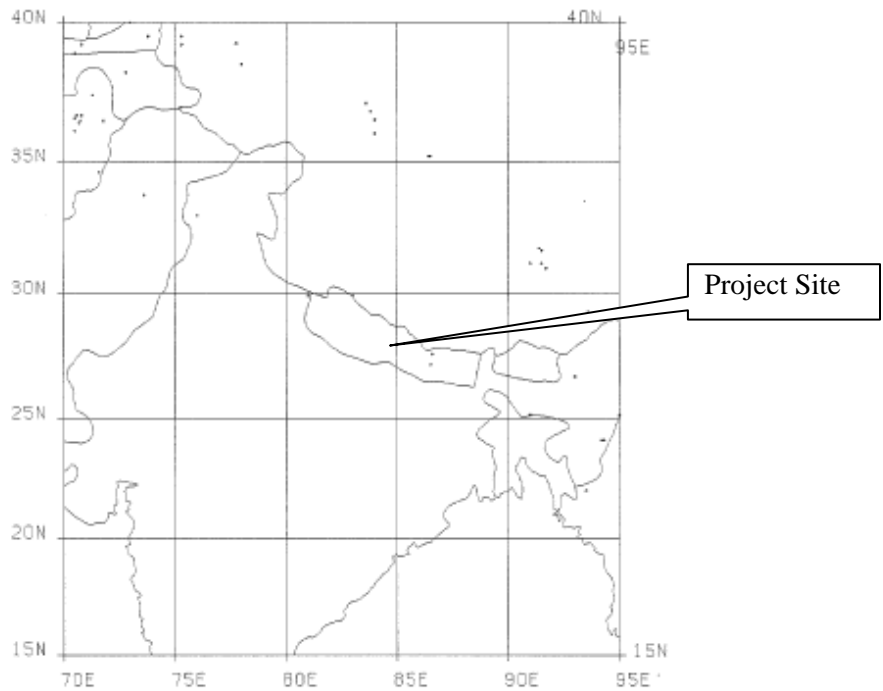


Fig. 8.2.1-6 Epicenter Distribution of Earthquakes of Magnitude more than 7

(2) Epicenter Distribution by Seismic Center Depth

Table 8.2.1-2 shows the occurrence frequency by seismic center depth among the collected seismic data.

Table 8.2.1-2 Occurrence Frequency of Seismic Center Depth among the Collected Data

Seismic Center depth (km)	Number of data	Amount	Regards
<6	113	113	Surface earthquake
<10	53	166	Crust floating earthquake
<20	333	499	
<40	2,915	3,414	
<60	401	3,815	
<80	158	3,973	
<100	42	4,015	
100>	45	4,060	
Total	4,060		

Figs. 8.2.1-7 to 8.2.1-14 show the seismic center depth distribution of the earthquakes listed in **Table 8.2.1-2** by depth. The following are summarized based on the epicenter distributions;

- Earthquakes with a seismic center depth of less than 10 km occurred nationwide at random.
- Earthquakes with a seismic center depth of more than 10 km occurred in the Himalayan tectonic zone.
- Earthquakes with a seismic center depth of more than 10 km did not occur near the project site.

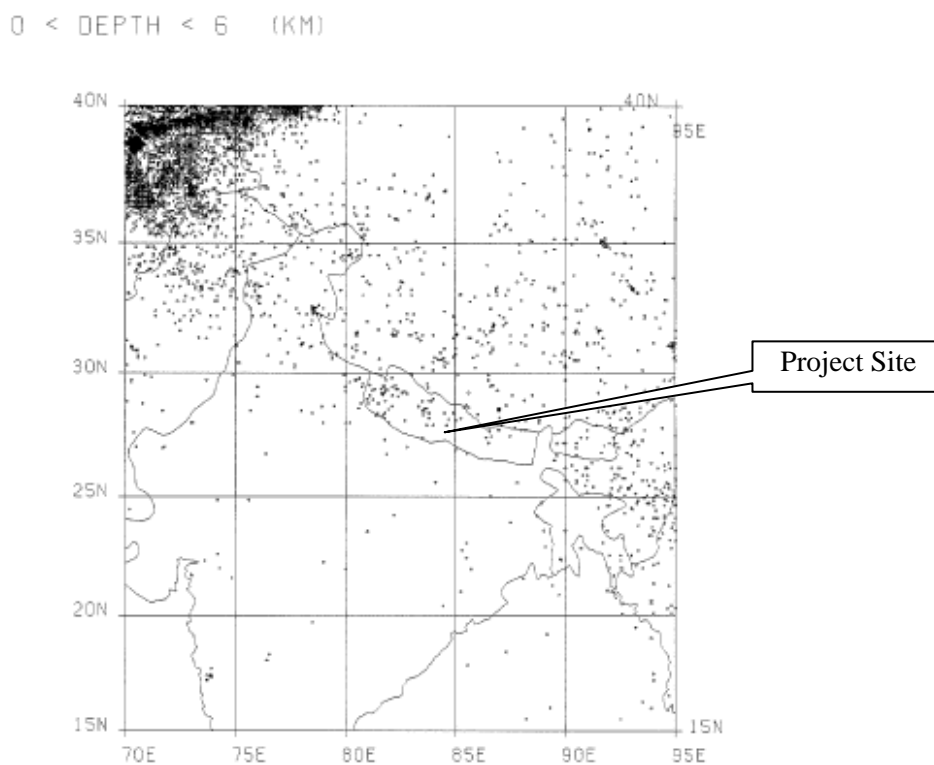


Fig. 8.2.1-7 Epicenter Distribution of Earthquakes less than 6 km in Depth

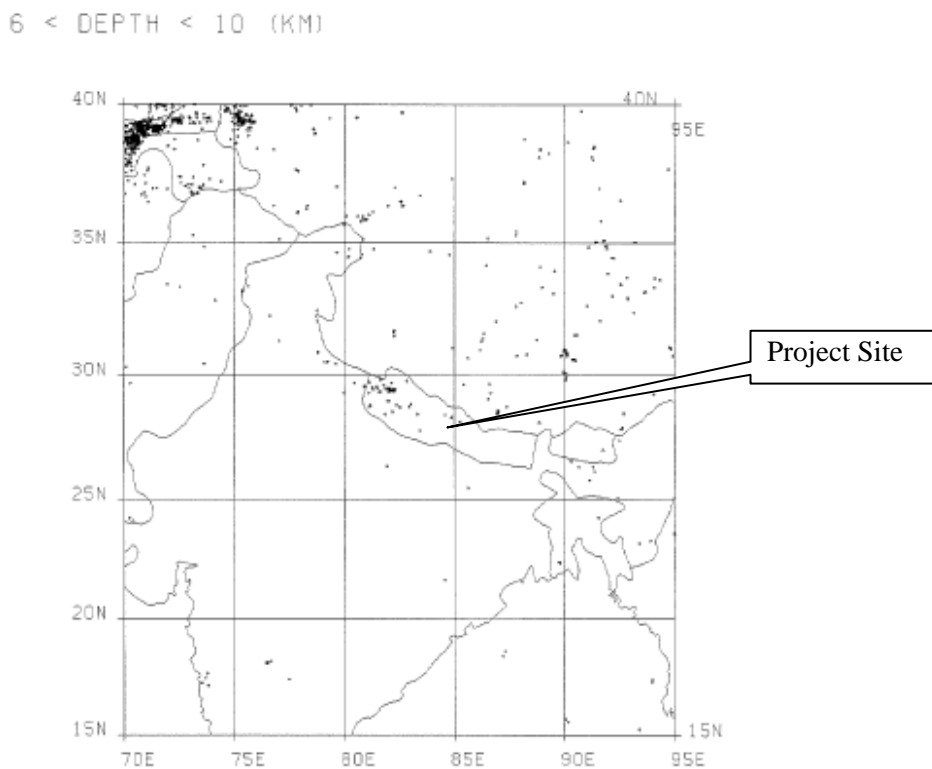


Fig. 8.2.1-8 Epicenter Distribution of Earthquakes between 6 and 10 km in Depth

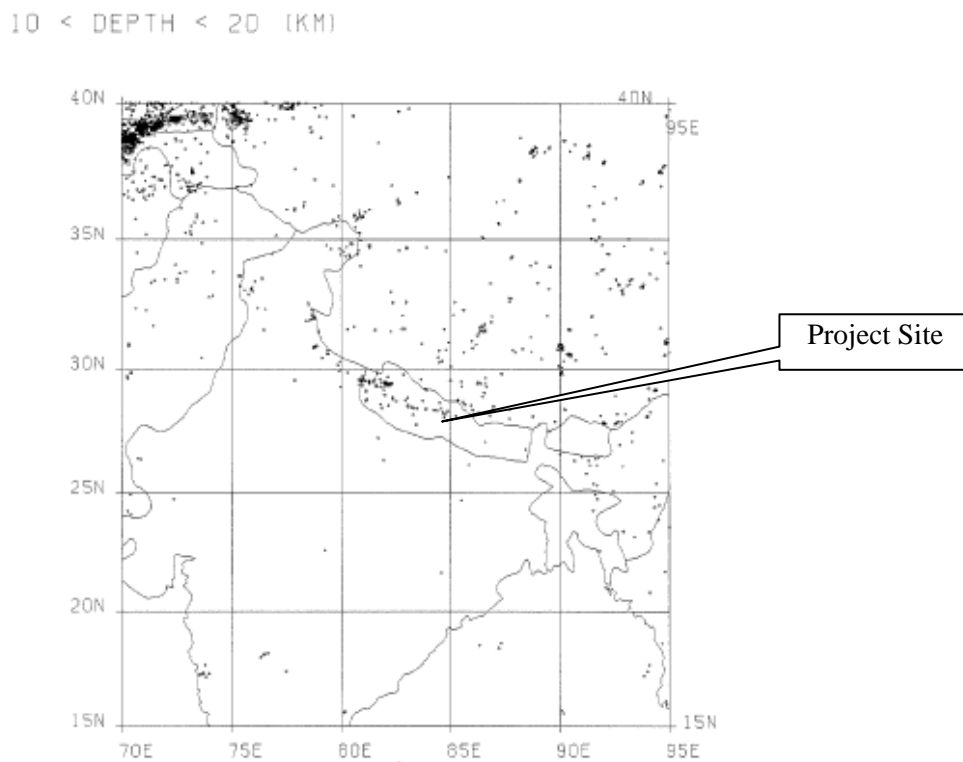


Fig. 8.2.1-9 Epicenter Distribution of Earthquakes between 10 and 20 km in Depth

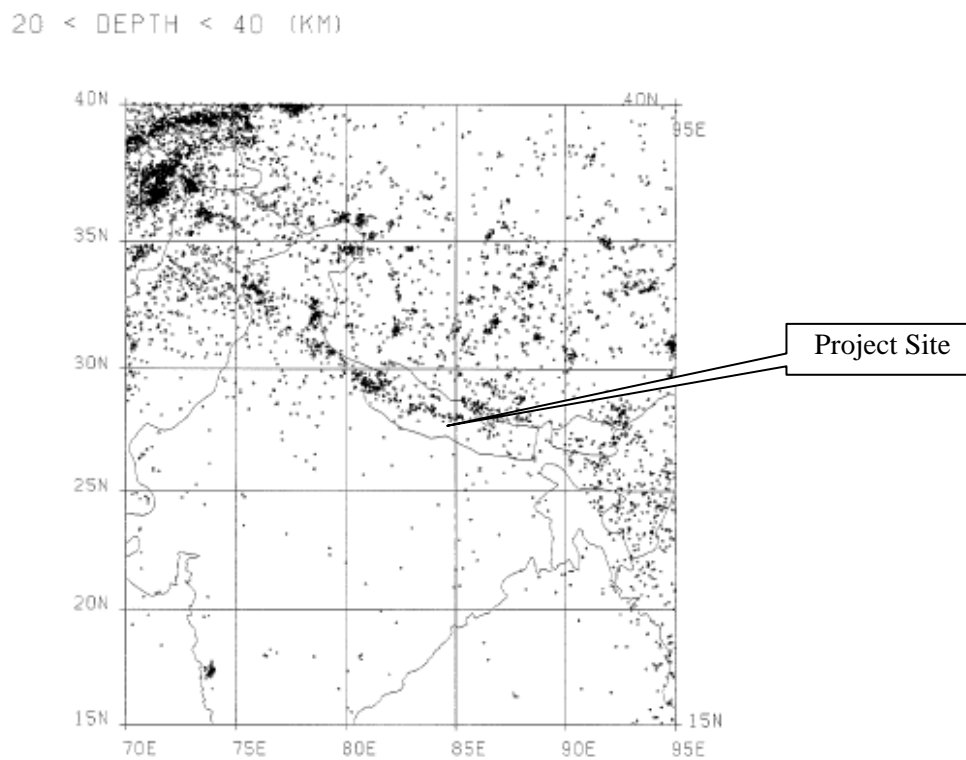


Fig. 8.2.1-10 Epicenter Distribution of Earthquakes between 20 and 40 km in Depth

40 < DEPTH < 60 (KM)

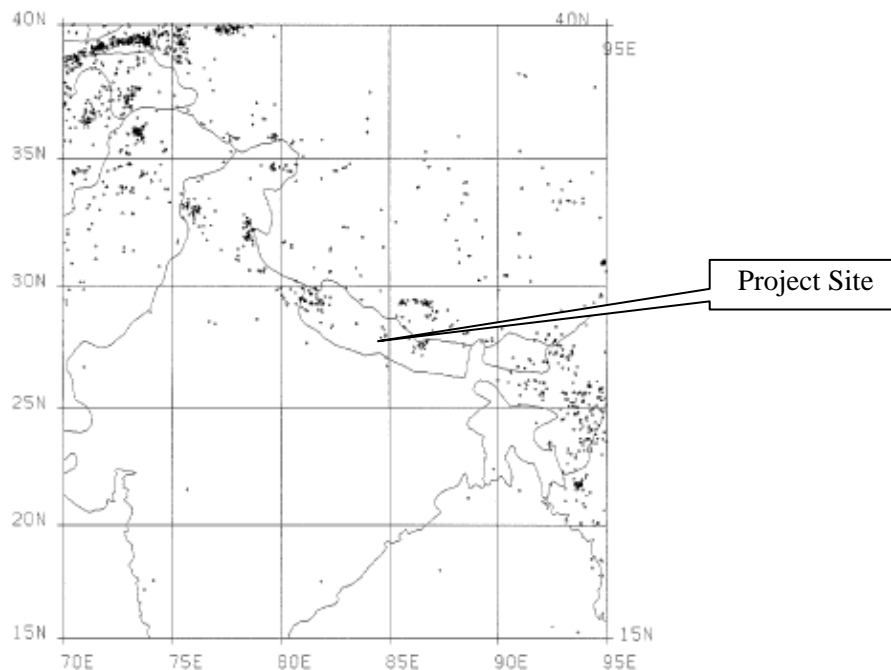


Fig. 8.2.1-11 Epicenter Distribution of Earthquakes between 40 and 60 km in Depth

60 < DEPTH < 80 (KM)

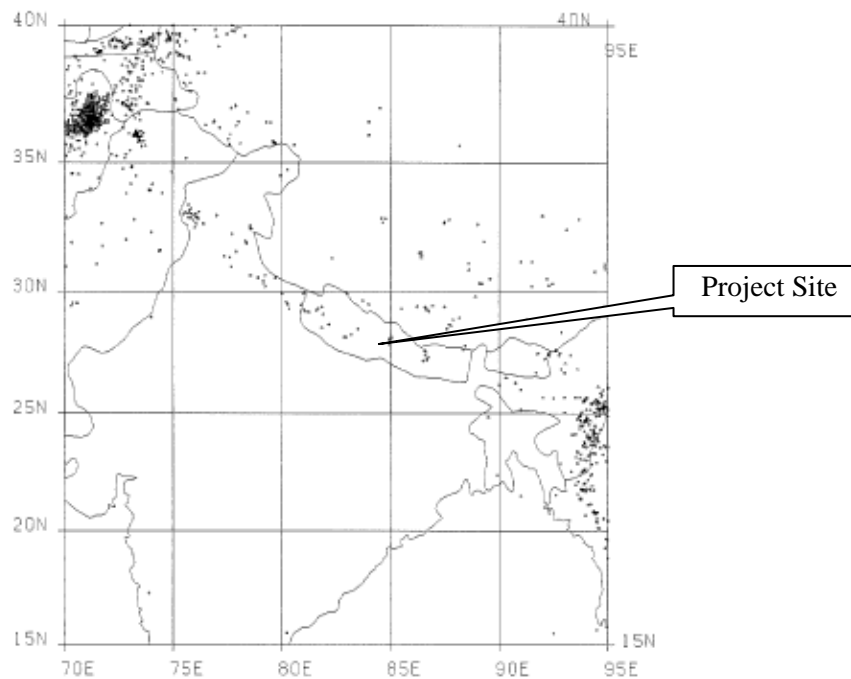


Fig. 8.2.1-12 Epicenter Distribution of Earthquakes between 60 and 80 km in Depth

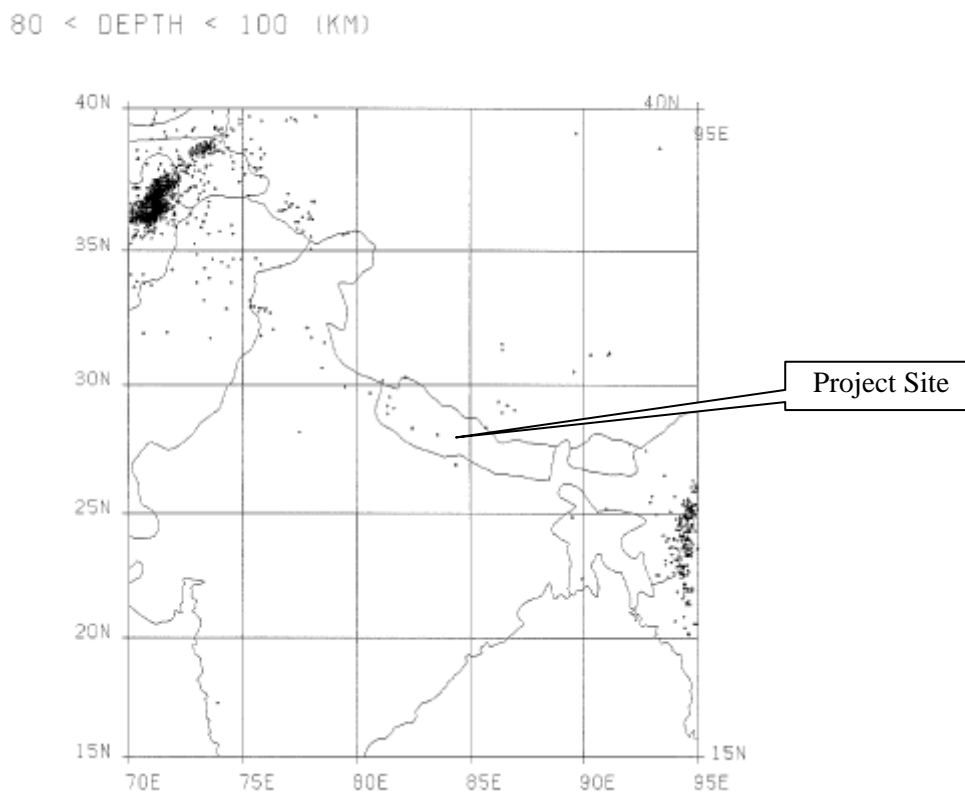


Fig. 8.2.1-13 Epicenter Distribution of Earthquakes between 80 and 100 km in Depth

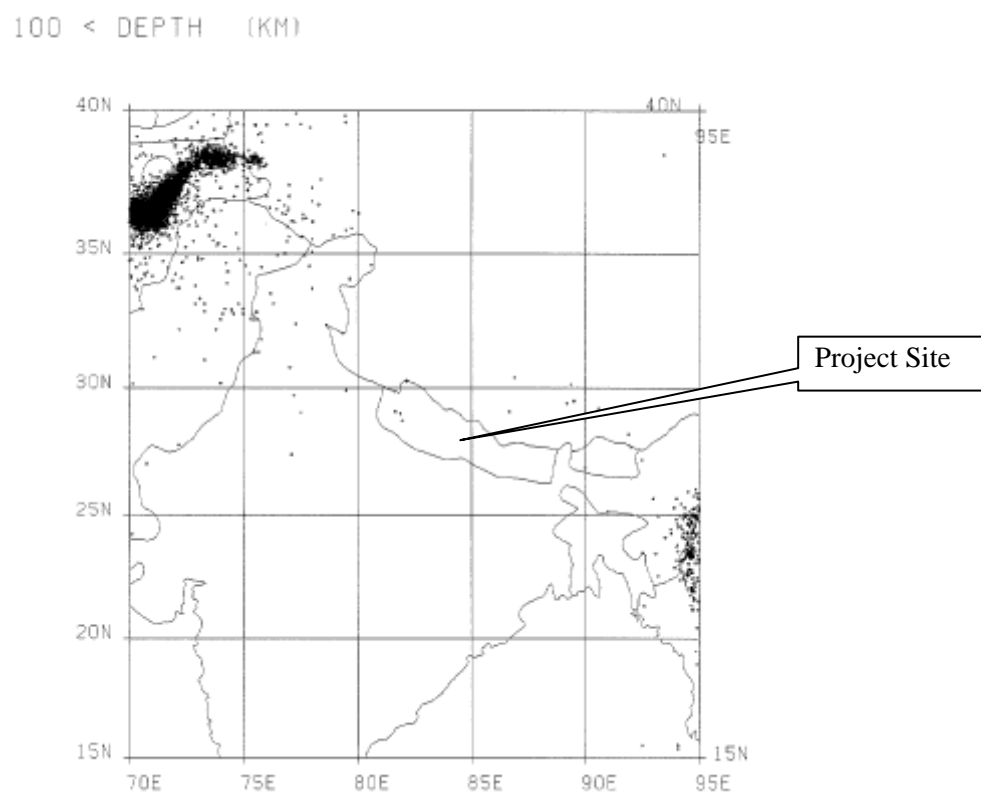


Fig. 8.2.1-14 Epicenter Distribution of Earthquakes more than 100 km in Depth

8.2.2 Estimation of Maximum Acceleration at the Dam Site

Of the previously proposed attenuation models (equations), which estimate the peak ground acceleration A (gal), in terms of the earthquake magnitude M, and the epicentral distance (km) or seismic central (km), the four models shown below are used in the Study in consideration of those applied to other similar studies:

$$\text{Log A} = 3.090 + 0.347 M - 2 \text{Log (R+25)} \dots\dots\dots (1)$$

By C. Oliveria

$$\text{Log A} = 2.674 + 0.278M - 1.301 \text{Log (R+25)}\dots\dots\dots (2)$$

By R. K. McGuide

$$\text{Log A} = 2.041 + 0.347 M - 1.6 \text{Log D} \dots\dots\dots (3)$$

By L. Esteva and E. Rosenblueth

$$\text{Log A} = 2.308 + 0.411 M - 1.637 \text{Log (R+30)}\dots\dots\dots (4)$$

By T. Katayama

The peak acceleration was calculated by using the above four attenuation models for all seismic data, and **Table 8.2.2-1** shows the annual maximum acceleration during the observation period.

Table 8.2.2-1 Annual Maximum Acceleration during Observation

YEAR	Attenuation Model 1		Attenuation Model 2		Attenuation Model 3		Attenuation Model 4	
	ACC.	LOG(ACC.)	ACC.	LOG(ACC.)	ACC.	LOG(ACC.)	ACC.	LOG(ACC.)
1905	0.69	-0.16079	9.41	0.97339	1.02	0.00763	4.46	0.64937
1906	0	0	0	0	0	0	0	0
1907	0	0	0	0	0	0	0	0
1908	0.69	-0.15969	8.34	0.92131	0.89	-0.05263	3.31	0.52025
1909	0	0	0	0	0	0	0	0
1910	0	0	0	0	0	0	0	0
1911	0.99	-0.00638	10.3	1.01267	1.16	0.06632	4.21	0.62398
1912	0	0	0	0	0	0	0	0
1913	4.26	-0.62993	27.95	1.44483	4.25	0.62832	15.27	1.18375
1914	0.24	-0.62765	3.99	0.60069	0.35	-0.45765	1.26	0.09966
1915	0.57	-0.24568	7.39	0.86851	0.76	-0.12038	2.87	0.4581
1916	2.48	-0.39449	20.17	1.3048	2.74	0.43735	10.63	1.02661
1917	0	0	0	0	0	0	0	0
1918	1.07	-0.02993	10.27	1.01172	1.18	0.07179	3.91	0.59229
1919	0	0	0	0	0	0	0	0
1920	0.22	-0.64826	3.79	0.57893	0.33	-0.48451	1.15	0.06233
1921	0.39	-0.41444	5.38	0.73102	0.51	-0.29175	1.79	0.25259
1922	0	0	0	0	0	0	0	0
1923	0.56	-0.25117	7.33	0.86494	0.75	-0.12493	2.84	0.45363
1924	0.61	-0.21767	7.37	0.86739	0.76	-0.11893	2.71	0.43312
1925	0	0	0	0	0	0	0	0
1926	0.21	-0.67881	3.62	0.55905	0.31	-0.50959	1.09	0.03745
1927	0.63	-0.20077	7.56	0.87838	0.79	-0.10484	2.8	0.44684
1928	0	0	0	0	0	0	0	0
1929	0	0	0	0	0	0	0	0
1930	0.75	-0.12674	8.83	0.94588	0.95	-0.02172	3.59	0.55476
1931	1.58	-0.19997	12.86	1.10926	1.61	0.2059	4.98	0.69682
1932	0.32	-0.49169	4.56	0.65934	0.42	-0.38012	1.37	0.13692
1933	0.33	-0.4851	4.61	0.66363	0.42	-0.37464	1.39	0.14228
1934	6.86	-0.83649	41.24	1.61532	6.9	0.8391	27.6	1.44096
1935	1.01	-0.00512	10.29	1.01231	1.17	0.06776	4.11	0.61384
1936	19.48	-1.28958	73.12	1.86406	17.16	1.23441	48.31	1.68405
1937	0.28	-0.55627	4.11	0.6142	0.37	-0.43723	1.25	0.09643
1938	1.6	-0.20454	12.86	1.1091	1.61	0.20721	4.93	0.69261
1939	0	0	0	0	0	0	0	0
1940	0.32	-0.49438	4.78	0.67902	0.44	-0.35784	1.54	0.18758
1941	0.43	-0.36297	5.94	0.7739	0.58	-0.23922	2.12	0.32587
1942	0	0	0	0	0	0	0	0
1943	0.4	-0.39448	5.96	0.77537	0.58	-0.23886	2.22	0.34604
1944	1.64	-0.21468	14.34	1.15647	1.79	0.25333	6.35	0.80298
1945	0.95	-0.02057	9.9	0.9956	1.11	0.04611	3.92	0.59302
1946	0.31	-0.51457	4.63	0.66589	0.42	-0.37449	1.48	0.17115
1947	0.97	-0.01278	9.82	0.9923	1.11	0.04399	3.79	0.57855
1948	0.22	-0.66286	3.71	0.56942	0.32	-0.4965	1.12	0.05044
1949	0	0	0	0	0	0	0	0
1950	0.24	-0.62571	4	0.60195	0.35	-0.45606	1.26	0.10124
1951	0.93	-0.03274	10.88	1.03682	1.23	0.08995	5.07	0.70469
1952	0.64	-0.19152	8.27	0.91733	0.87	-0.05998	3.43	0.53564
1953	2.74	-0.4373	18.22	1.26051	2.59	0.41304	7.58	0.87957
1954	28.75	-1.45869	90.75	1.95786	26.07	1.41615	59.29	1.77296
1955	2.15	-0.33207	15.85	1.1999	2.12	0.32538	6.53	0.81499
1956	0.53	-0.27544	6.6	0.81967	0.66	-0.17938	2.34	0.36907
1957	3.69	-0.56722	23.88	1.37796	3.57	0.55252	11.68	1.06737
1958	8.02	-0.90435	37.7	1.57635	7.11	0.85189	19.17	1.28261
1959	0.39	-0.40423	5.49	0.73923	0.52	-0.28151	1.84	0.26475
1960	1.37	-0.13587	11.6	1.06443	1.4	0.14751	4.34	0.63729
1961	1.62	-0.21042	13.16	1.1192	1.65	0.21771	5.17	0.71313
1962	10.38	-1.01606	41.71	1.62027	9.22	0.96491	19.7	1.29456
1963	0.78	-0.10772	7.35	0.86624	0.8	-0.09876	2.19	0.34115
1964	1.49	-0.17372	11.81	1.07232	1.47	0.16646	4.22	0.62563
1965	7.46	-0.87274	35.74	1.55317	6.62	0.82083	17.81	1.25077
1966	14.57	-1.16332	51.2	1.70926	13.5	1.13042	24.58	1.39054
1967	1.72	-0.2366	12.89	1.11009	1.66	0.21968	4.66	0.66819
1968	2.47	-0.39302	16.29	1.21184	2.29	0.36028	6.22	0.79347
1969	15.24	-1.18291	52.72	1.722	14.22	1.15292	25.45	1.40566
1970	11.72	-1.06894	44.45	1.64787	10.59	1.02494	20.77	1.31745
1971	3.5	-0.54409	19.21	1.28345	3.1	0.49069	6.99	0.84475
1972	0.93	-0.03358	8.3	0.91917	0.93	-0.0302	2.59	0.4127
1973	3.01	-0.47854	17.66	1.24708	2.69	0.42964	6.44	0.80913
1974	3.47	-0.54078	20.1	1.30325	3.12	0.49429	7.93	0.89917
1975	12.9	-1.1106	46.63	1.66869	11.92	1.07616	21.51	1.33266
1976	1.76	-0.24544	11.87	1.07454	1.59	0.20243	3.71	0.56975
1977	0.78	-0.10522	7.83	0.89401	0.85	-0.07256	2.56	0.40866
1978	13.77	-1.13903	48.08	1.68196	13.01	1.11434	21.89	1.34024
1979	8.38	-0.92331	30.49	1.48413	8.66	0.93737	10.35	1.01509
1980	1.63	-0.21335	14.05	1.14776	1.76	0.2446	6.06	0.78232
1981	11.6	-1.06462	39.06	1.59173	12.32	1.09057	14.88	1.16663
1982	2.73	-0.43643	15.06	1.17787	2.41	0.38127	4.64	0.66645
1983	3.16	-0.4996	16.76	1.22419	2.78	0.44468	5.37	0.72994
1984	5.99	-0.77717	26.02	1.41536	5.49	0.73996	10.49	1.02098
1985	2.53	-0.40327	14.51	1.16153	2.23	0.34851	4.51	0.65411
1986	14.68	-1.16664	55.17	1.74174	13.04	1.11519	29.86	1.47515
1987	14.02	-1.14689	50.8	1.70589	12.76	1.10586	25.84	1.41226
1988	20.16	-1.30453	63.87	1.8053	19.58	1.29176	32.41	1.51069
1989	10.5	-1.02114	36.6	1.56345	10.8	1.03332	13.6	1.13363
1990	3.88	-0.58924	19.4	1.28773	3.43	0.53549	6.52	0.81414
1991	1.21	-0.08372	8.99	0.95366	1.11	0.04507	3.51	0.54499
1992	1.23	-0.08871	9.83	0.99258	1.16	0.06586	3.24	0.51022
1993	5.26	-0.72096	25.09	1.39955	4.64	0.66623	9.7	0.98687
1994	3.61	-0.55714	17.72	1.24855	3.22	0.50755	5.5	0.74013
1995	12.65	-1.10211	42.63	1.62971	12.93	1.11159	17.12	1.23345
1996	17.15	-1.23431	50.12	1.70003	22.05	1.34335	19.41	1.28809
1997	6.99	-0.84438	32.92	1.51747	6.16	0.7899	15.25	1.18326
1998	4.24	-0.62754	24.08	1.38165	3.85	0.58499	10.59	1.02486
1999	7.2	-0.85721	28.25	1.45106	6.9	0.83879	10.8	1.03324
2000	2.78	-0.44333	15.87	1.20065	2.45	0.38954	5.25	0.71999
2001	25.83	-1.4122	78.28	1.89364	24.92	1.39653	44.05	1.64398
2002	6.07	-0.78296	24.65	1.39178	5.81	0.76427	8.15	0.91137
2003	7.91	-0.89832	32.53	1.51231	7.14	0.85361	13.13	1.11842
2004	9.6	-0.98205	36.04	1.55684	9.05	0.95662	14.32	1.15609

In **Table 8.2.2-1**, the acceleration in 1954 derived from Eq. (5) is the largest of all. The earthquake corresponding to this acceleration occurred on September 4, 1954 and had a magnitude of 6.6, an epicenter distance from the project site of 59 km, and a seismic center depth of 30 km. This acceleration by Eq. (5) is larger than the results obtained from the other equations.

Estimation of the maximum acceleration for certain return periods was carried out based on stochastic theory. Although the probability function of the maximum acceleration remains unknown, it is reasonable to presume that the function should be associated with the third asymptotic distribution function. The results of calculation by each attenuation model are shown in **Figs. 8.2.2-1 ~ 8.2.2-4**. **Table 8.2.2-2** summarizes the maximum accelerations by each attenuation model for return periods of 50 years, 100 years, 200 years, 300 years, 500 years, 1,000 years, and 10,000 years.

Table 8.2.2-2 Maximum Acceleration Value by Each Equation to the Advent Period

MAIN-CURVE

NO.	Return Period	Probability	Attenuation 1	Attenuation 2	Attenuation 3	Attenuation 4
1	50	0.98	32.5316	78.4983	23.0424	38.7179
2	100	0.99	42.9713	91.5436	28.1659	45.4992
3	150	0.9933333	49.3353	98.6746	31.0141	49.1623
4	200	0.995	53.8979	103.4791	32.9455	51.6087
5	300	0.9966667	60.325	109.8698	35.5243	54.8318
6	500	0.998	68.3022	117.268	38.5155	58.5133
7	1000	0.999	78.6862	126.1414	42.0955	62.847
8	10000	0.9999	107.2284	147.0039	50.3481	72.5741

REFERENCE-CURVE

NO.	Return Period	Probability	Attenuation 1	Attenuation 2	Attenuation 3	Attenuation 4
1	50	0.98	21.3023	75.2575	20.6293	47.5956
2	100	0.99	26.943	87.4151	24.9746	56.9454
3	150	0.9933333	30.2738	94.0416	27.3733	62.0627
4	200	0.995	32.6204	98.4988	28.9939	65.504
5	300	0.9966667	35.8743	104.4197	31.1507	70.0657
6	500	0.998	39.8387	111.2629	33.6429	75.3129
7	1000	0.999	44.8933	119.4556	36.6137	81.5363
8	10000	0.9999	58.2942	138.6613	43.4174	95.6761

The result by the attenuation model (2) are larger than those obtained by the models.

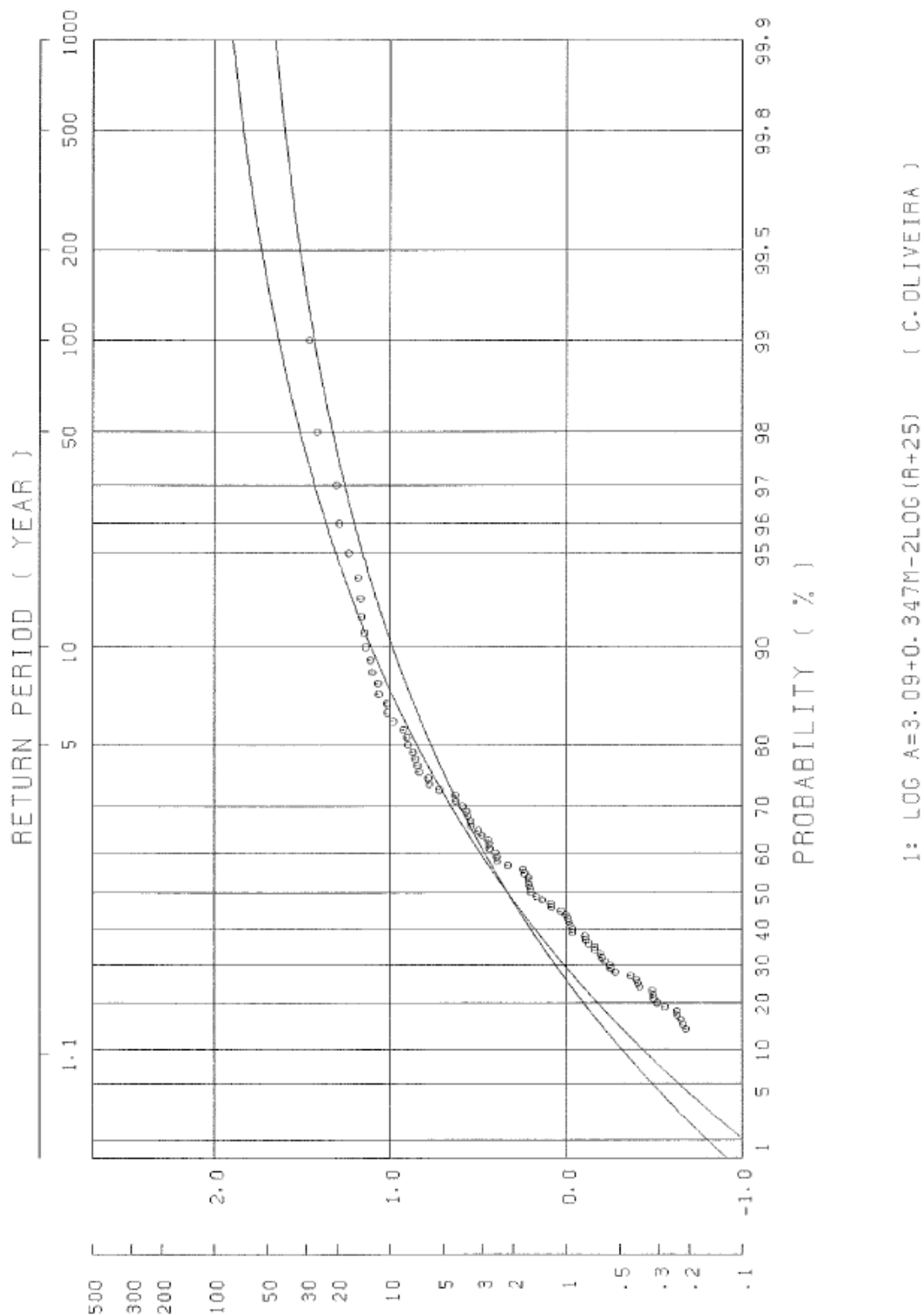
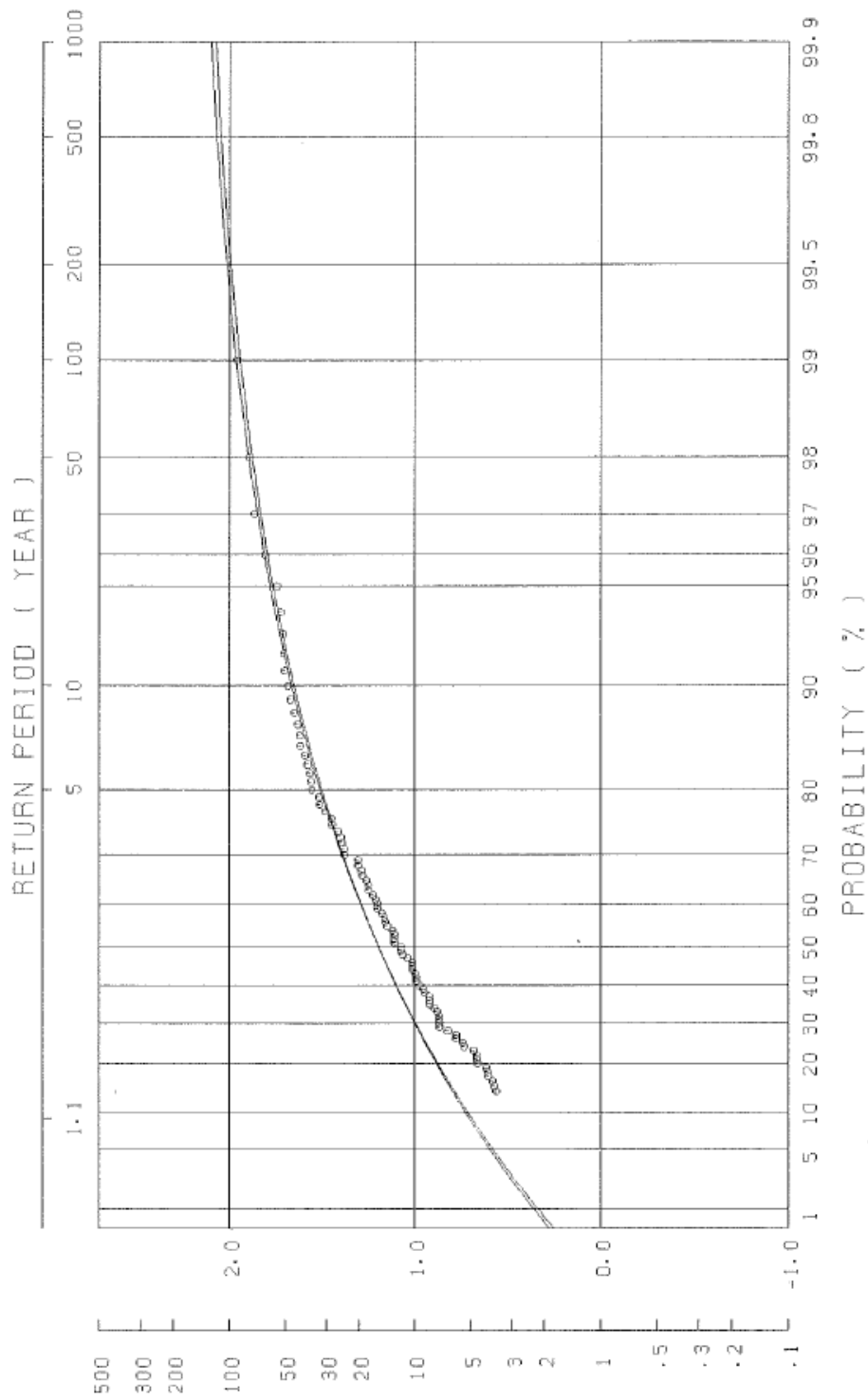


Fig. 8.2.2-1 Maximum Acceleration for the Return Period by Equation (1)



(R. K. MCGUIRE)

Fig. 8.2.2-2 Maximum Acceleration for the Return Period by Equation (2)

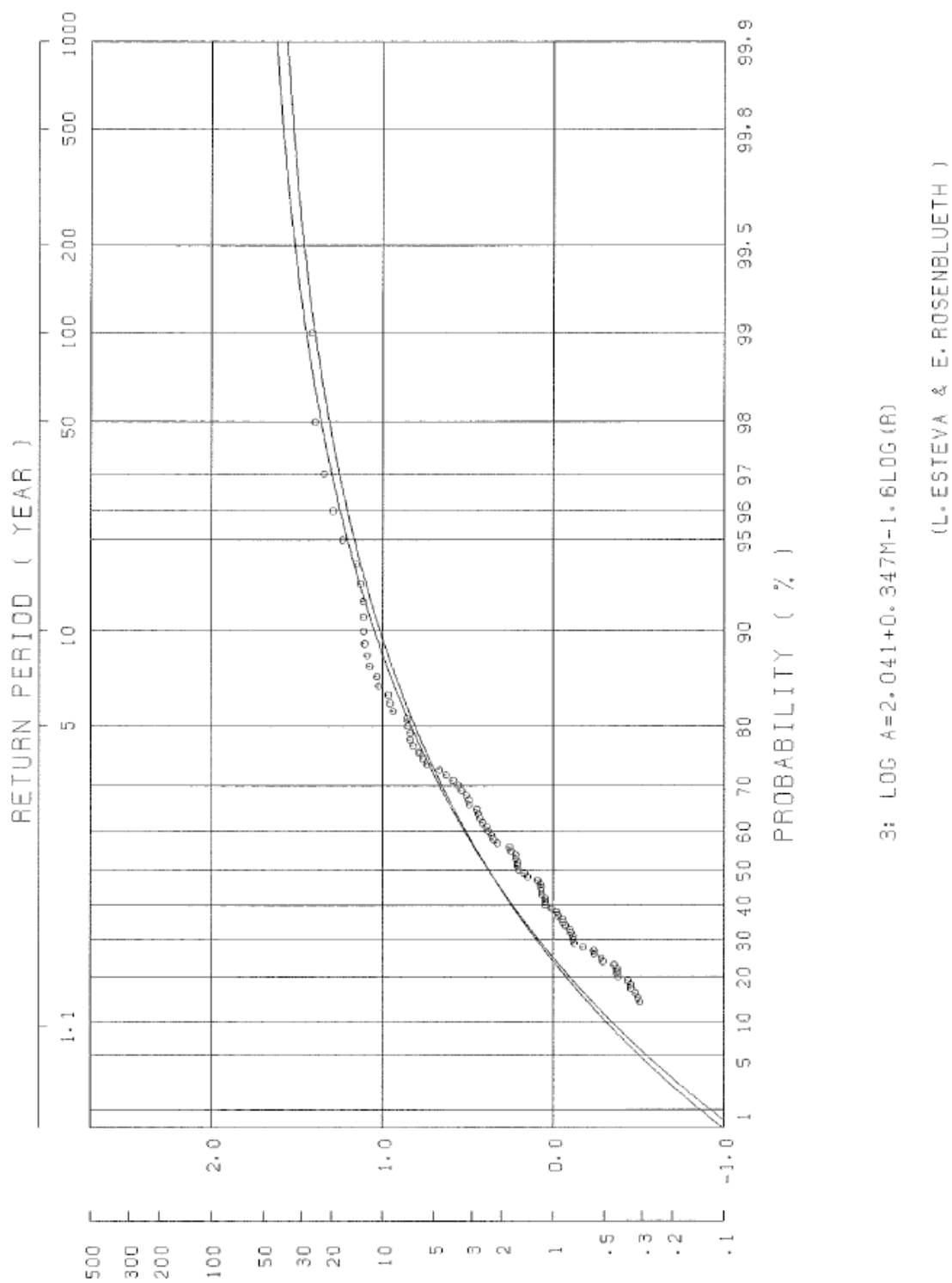
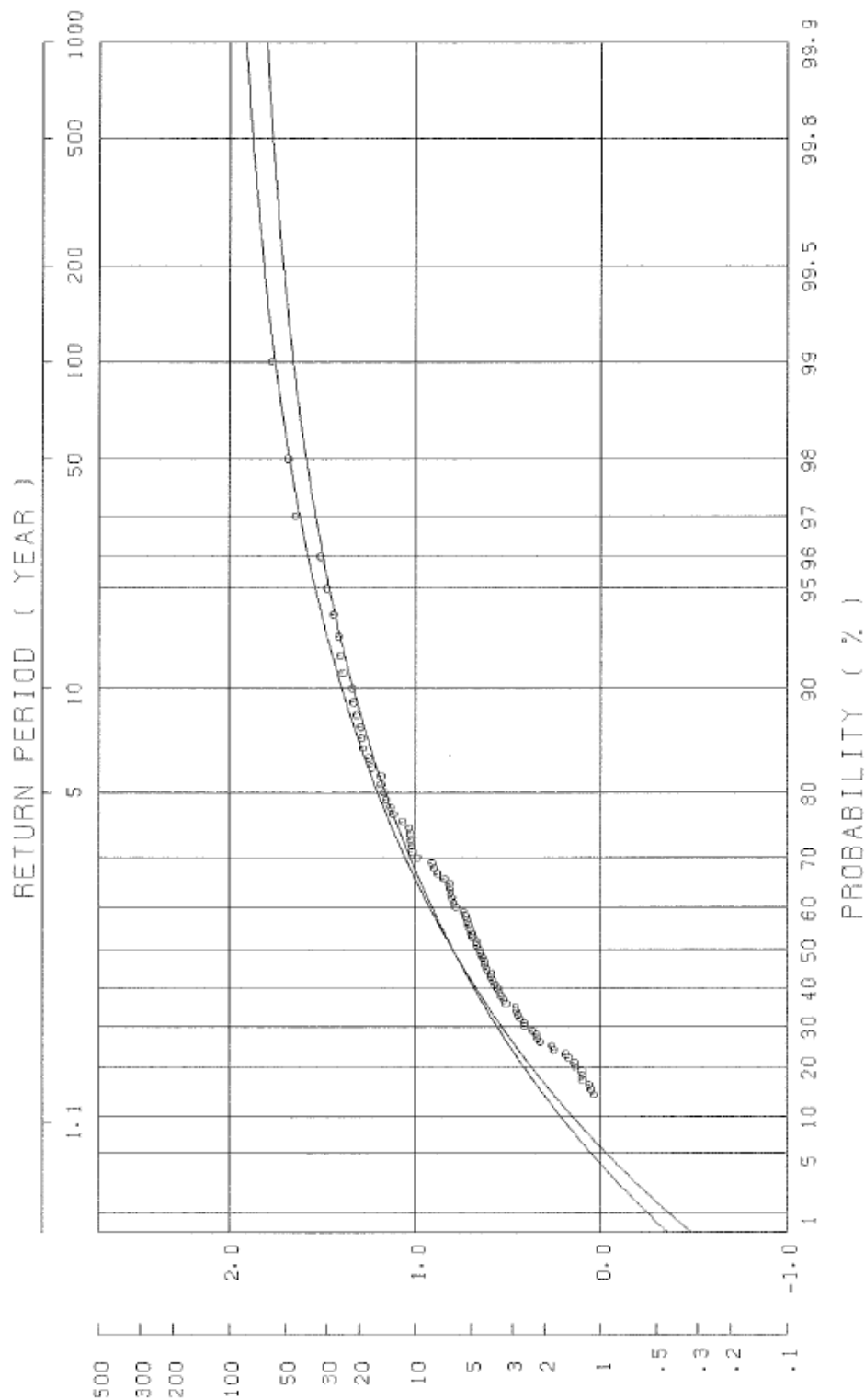


Fig. 8.2.2-3 Maximum Acceleration for the Return Period by Equation (3)



4: $\text{LOG } A = 2.308 + 0.411M - 1.637\text{LOG}(R+30)$

(T. KATAYAMA)

Fig. 8.2.2-4 Maximum Acceleration for the Return Period by Equation (4)

8.2.3 Design Horizontal Seismic Coefficient

(1) Evaluation Based on the Seismic Design Code in Nepal

The Seismic Design Code in Nepal is based on the seismic risk map shown in **Fig. 8.2.3-1**. In order to determine the seismic coefficient, the country is divided into three seismic risk zones, and structural foundations are also classified into three categories, based on the permissible bearing capacity of the foundation.

The Upper Seti Project site is located in the second seismic risk zone (Zone II), and the foundation of the dam belongs to “Hard Rock”, meaning the basic horizontal seismic coefficient is considered to be 0.05. In the case of dams, the importance factor should be taken as 1.5. Consequently, the horizontal seismic coefficient for the Upper Seti dam can be evaluated as 0.075.

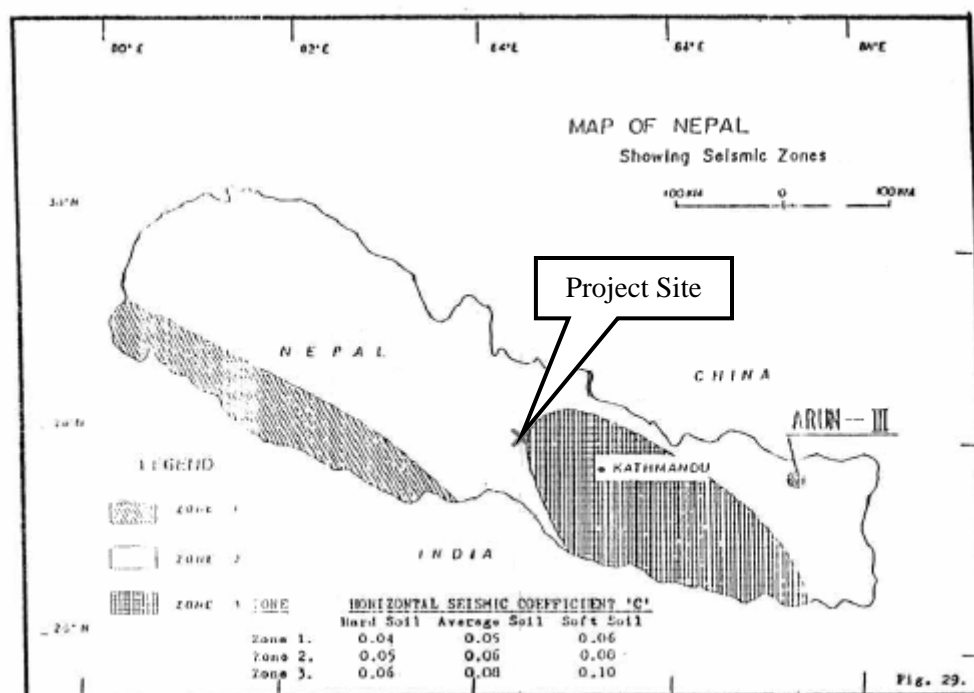


Fig. 8.2.3-1 Seismic Hazard Map in Nepal

(2) Evaluation Based on the India Standard

The seismic risk map in the Indian Criteria for the Earthquake Resistant Design of Structures is shown in **Fig. 8.2.3-2**. According to the Indian Standard, the country is divided into five seismic risk zones. The third seismic risk zone of Nepal (Zone III) can be considered to correspond to the fifth seismic risk zone of India, in comparison with both risk maps (see **Figs. 8.2.3-1** and **8.2.3-2**). Hence, the Upper Seti Project site is located in the Indian Standard’s fourth seismic risk zone, because the site is located in the Nepalese second seismic risk zone,

which is lower than the third seismic risk zone. As shown in **Table 8.2.3-1**, the basic horizontal seismic coefficient is 0.05.

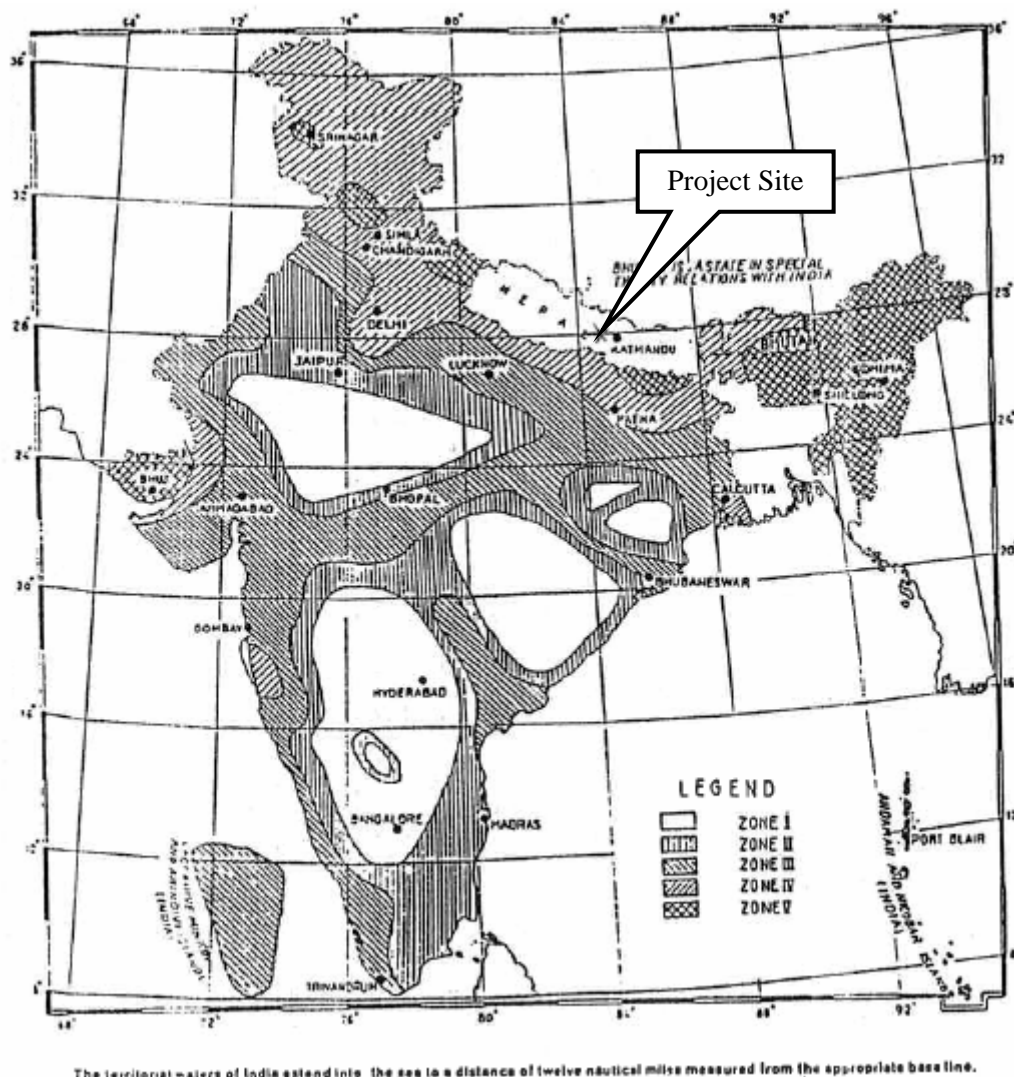


Fig. 8.2.3-2 Seismic Hazard Map in India

According to the Indian Standard, the horizontal seismic coefficient is defined as the following equation:

$$\alpha_h = \beta * I * \alpha_0$$

- where
- α_h : Design horizontal seismic coefficient
 - B : Foundation factor
 - I : Importance factor
 - α_0 : Horizontal seismic coefficient

It is suggested that the value of the foundation factor β for dams should be taken as 1.0 and that the value of the importance factor I should be taken as 2.0. Consequently, the Design

horizontal seismic coefficient for the Upper Seti Dam is evaluated as 0.10.

Table 8.2.3-1 Basic Seismic Coefficient in the Indian Seismic Hazard Region

Seismic hazard region	Basic horizontal seismic efficient
V	0.08
IV	0.05
III	0.05
II	0.02
I	0.01

(3) Evaluation of Maximum Acceleration

Table 8.2.3-2 summarizes the results of estimation of the maximum accelerations, due to historical earthquakes and of the probability analysis.

Table 8.2.3-2 Summary of Maximum Acceleration Estimation at the Upper Seti Dam Site

	Date	Location	LAT(N)	Long(E)	M	R	Depth	D	Eq.(1)	Eq.(2)	Eq.(3)	Eq.(4)	Remarks	
Historical Damaging Earthquake	18970612	Assam	22.5	91.8	8.7	1036.04	1.6	1036.04	1.14	14.33	1.72	1.14		
	19050404	Kangra	33	76	8.6	1077.32	19	1077.49	0.98	12.78	1.49	0.98		
	19081212	Burma	26.5	97	7.5	1427.57		1427.57	0.23	4.42	0.39	0.23		
	19180708	Assam	24.5	91	7.6	843.22		843.22	0.71	9.20	0.99	0.71		
	19340112	Bihar	26.5	86.5	8.4	297.43		297.43	9.73	55.68	9.96	9.73		
	19350530	Quetta	29	66.7	7.6	1958.00	11	1958.04	0.14	3.14	0.26	0.14		
	19470729	NE Assam	28.5	94	7.9	1086.12	30	1086.53	0.55	8.08	0.84	0.55		
19500815	Assam	28.5	96.7	8.7	1386.31	1.526	1386.31	0.65	9.88	1.08	0.65			
Near Field Earthquakes around Site	19540904		28.3	83.8	6.6	59.188	30	66.357	28.75	90.75	26.07	59.29	Max data	
	19960127		28.067	84.267	4.5	12.63	22	25.37	31.66	51.35	22.68	17.67		
	20010716		27.967	84.717	5.9	51.08	20	54.86	23.70	69.07	20.21	21.51		
Return Period (year)			Probability (%)											
50			98.0%							32.53	78.50	23.04	38.72	Main Curve
100			99.0%							42.97	91.54	28.17	45.50	
200			99.5%							53.90	103.48	32.95	51.61	
50			98.0%							21.3023	75.2575	20.6293	47.5956	Reference Curve
100			99.0%							26.943	87.4151	24.9746	56.9454	
200			99.5%							32.6204	98.4988	28.9939	65.504	

To convert the maximum acceleration of earthquake motion into a design seismic coefficient, the following method is applied:

$$eff = R * \alpha = R * Amax / 980$$

α_{eff} : Effective design seismic coefficient

R : Reduction factor (The empirical value of R is approximately 0.55 to 0.65)

Reasons to consider R are described below:

- The static analysis method is that used to evaluate stresses and deformations by inputting static inertia force to an analytical model as an earthquake force. In other words, the static analysis method can be considered a kind of dynamic analysis method involving

the input of the harmonic waves of frequency = infinite as a design input motion or earthquake force. Accordingly, if R is not considered, such method overestimates the design seismic coefficient.

- Consideration of R was proposed based initially on empirical knowledge. However, similar results have also been reported in studies on dynamic and static analysis.

The horizontal seismic coefficient based on the above method is shown below and is estimated as 0.06.

Table 8.2.3-3 Seismic Coefficient Based Upon Maximum Acceleration

Estimated Value	Basis of Estimation
R = 0.6	The estimated maximum acceleration by statistical analysis is controlled by near-field earthquakes. Near-field earthquakes → Excel in high frequency → High reduction
Amax = 97.12 gal	a. Maximum acceleration of historical earthquakes by attenuation models 90.75 gal on September 4, 1954 by Eq. (2) b. Statistical Analysis 103.48 gal: by Eq. (2) Amax is estimated as the average of a. to b.
$\alpha_{eff} = 0.06$	$\alpha_{eff} = R * A_{max} / 980 = 0.06$

(4) Evaluation of Maximum Acceleration based on the Seismic Hazard Map of Nepal

The Seismic Hazard Map of Nepal, as shown in **Fig 8.2.3-3**, was obtained during the Site survey. According to this map, the Maximum Acceleration at the project site can be evaluated, and thus the value is evaluated as 230 gal.

Based upon this, the horizontal seismic coefficient based on the method as shown in (3) is shown below and estimated to be 0.15.

$$\begin{aligned}
 \alpha_{eff} &= R * \alpha = R * A_{max} / 980 \\
 &= 0.6 * 230 / 980 \\
 &= 0.1408 \Rightarrow 0.15
 \end{aligned}$$



Fig. 8.2.3-3 Seismic Hazard Map in Nepal

(5) Design Horizontal Seismic Coefficient for the Upper Seti Project

The values of the design horizontal seismic coefficient estimated different process are summarized in **Table 8.2.3-4**. It is concluded in the Study that the design horizontal seismic coefficient for the Upper Seti dam should be taken as 0.15.

Table 8.2.3-4 Result of Seismic Coefficient Estimation obtained in Various Ways

Evaluation Basis	Design Horizontal Seismic Coefficient
Seismic Design Code in Nepal	0.075
The India Standard	0.10
Estimate based on Earthquake data records	0.06
Estimate based on the Nepalese Hazard Map	0.15
Proposed value for the Upper Seti Dam	0.15